…dedicated to Alessandro, Letizia and Davide…

XXXIII CYCLE OF PhD course in LIFE-SCIENCE AND BIOTECHNOLOGY

FLUORESCEIN GUIDED SURGERY FOR RESECTION OF CENTRAL AND PERIPHERAL NERVOUS SYSTEM TUMORS WITH YELLOW 560 nm SURGICAL MICROSCOPE FILTER

Dr.ssa Elena Beretta

Matricola: 733849

Corso di Studi: Scienze della vita e Biotecnologie

Docente guida: Prof. Paolo Castelnuovo

Tutor: Prof. Sergio Balbi.

Sede:

-Prof. Sergio Balbi DBSV presso Dipartimento di Neurochirurgia Ospedale di Circolo e Fondazione Macchi, via Guicciardini 9, Varese. Tel. 033278388/9

-Policlinico di Monza, Dipartimento di Neurochirurgia, Via Amati 111, Monza. Tel. 0392810234/732

ACKNOWLEDGEMENTS

I would first like to thank my supervisor Professor Paolo Castelnuovo and Professor Davide Locatelli that give me the opportunity to complete my study and my research during these years.

I would also like to thank my tutor, Professor Sergio Balbi, for his valuable guidance throughout my studies and for his support in formulating the research questions and suggestion in the writing process.

I will not forget to thank the operator theatre staff, my colleagues for their collaboration.

I'm thankful to the Institution Policlinico di Monza that give me the opportunity to go on with my project and tp my Chief Dr. Michele Incerti

I also remain grateful and thankful to my 'V drug', who pushed me and inspired me in this adventure, for his support and happy distractions for my mind outside of my research. I can't go on without…The best man I've never met.

In addition, I would like to thank my children for their curiosity, their will to give me help and for their funny experiments. Without their encouragements these years, it would be impossible for me to complete the research.

And a thank to my life, with all its trouble, chaos and lies. I try to make the worst seem better everyday.

Index

Introduction

Malignant brain tumors occur each year in 6-7 cases every 100,000 people in the US. The greatest survival benefit is observed in patients with complete resection of enhancing tumor. Removal of the final part of the neoplasm carries the greatest impact from an oncological point of view but also the greatest risk for neurological impairment. However, a complete tumor removal is not always feasible because of difficulties in recognizing tumor tissue at the tumor margin and infiltration of presumed motor eloquent area, based on pre-operative MR images with contrast.

Advances in fluorescence imaging over the past half-century have revolutionized the field of biological research. Fluorophores have become an integral part of modern laboratory work, enabling the visualization of biomolecules and cellular processes[1]. Fluorescence-guided surgery (FGS) relies on the accumulation of an administered fluorescent dye and visualization of the fluorescence signal during surgery [2].

Sodium-fluorescein (Na-Fl), the sodium salt of fluorescein, has the capability to accumulate in a specific cerebral area as a result of a leakage from a blood-brain barrier disruption, as happens in high-grade gliomas (HGG) and metastasis. Also, it accumulates in the peripheral area of the nervous system where a high and pathological vascularity is present.

The Fluorescein is an organic fluorescent dye with a peak excitation at 490 nm and emission between 500 and 550 nm. This dye in association with the use of optical filters centered on the peak's wavelength of excitation and emission demarcates the tumor tissue

during surgery maximizing the extent of resection of the tumors, allowing a longer survival and improving patients' prognosis[3,4].

The study highlights the benefit of combination of fluorescein and blue 490 nm and yellow 560 nm filter in optimizing the fluorescein dose necessary, reducing side effects and in optimizing the oncological benefit, improving patients' prognosis[3].

The aim of this work is evaluate the use of the Fluorescein in a comparative fashion between the different pathologies and quantify the intensity of Fluorescein in the microscopic view to detect a range in which we are sure to have pathological tissue. A threshold curve can reduce the probability of the unexpected residual tumor after surgery because of the absence of a clear residual intraoperative fluorescent tissue at the normal eye.

Principles of Fluorescence

FGS is fundamentally based on the detection of light produced by a fluorescent molecule that accumulates within a lesion. This is a method to distinguish the tumor tissue from the normal tissue (Fig. 1).

Fig.1 Tumor localization

A. Absent fluorescein staining in the lesion under illumination by the white light, captured just prior to Yellow 560 excitation. B. distinctive yellow-green staining was visible under illumination with yellow 560 filter.

A.

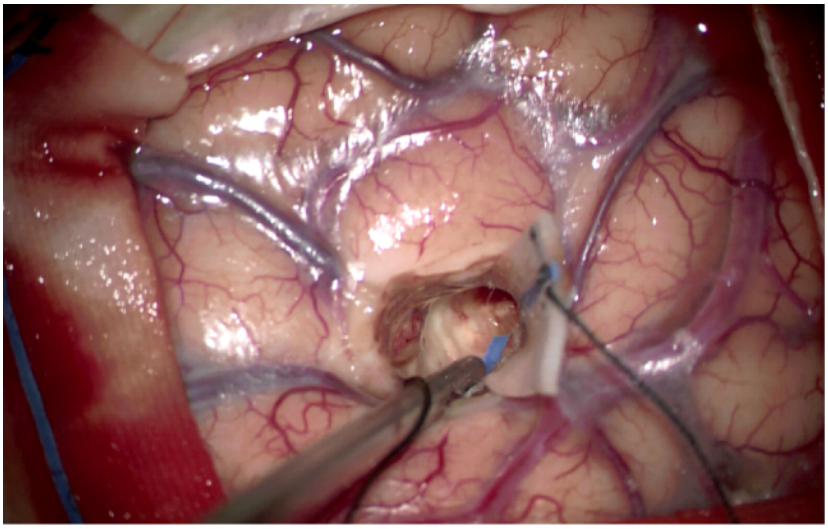

B.

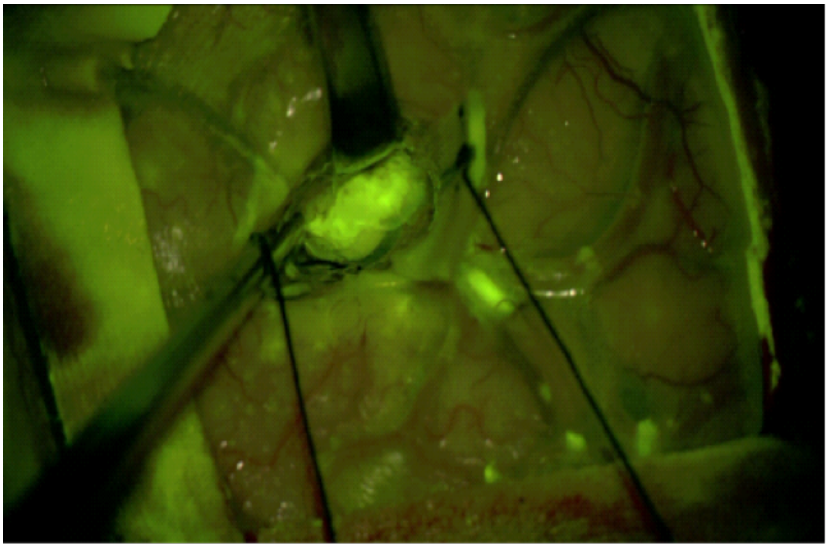

When any object is illuminated by white light, including wavelengths of visible spectrum (400-700nm), the object absorbs certain wavelengths of light and reflect others. Upon illumination of the brain parenchyma by a white light, the exposed tissue may be perceived as yellow. That is why brain tissue has the property of absorbing violet-blue light and reflecting yellow light.

Upon exposure to light, the absorbing molecule is excited from its ground state (S0) to an excited state (S1). The wavelengths of light absorbed correspond to the energy gap between S0 and S1. The chromophore may then return to the ground state by releasing the energy as heat.

The process of fluorescence is similar. The light is absorbed and excites the fluorophore to S1 state. It decays to S0 by releasing a portion of the energy as light, detected as fluorescence [2].

The stokes shift is the difference between the wavelengths of maximal light absorption and emission. Most fluorophores emit longer wavelengths light than they absorb. The fluorophore is excited from the S0 to the S1 state. It emits light as fluorescence and returns to S0, it arrives with a suboptimal geometry for S0 and undergoes relaxation to the optimal arrangement for S0 with concomitant release of energy as heat. The initially-absorbed energy is released in part by heat and in part by light with, leading to emission of lower energy and longer wavelength light. Fluorescein has a stoke shift of 26 nm[5].

Stokes shift allows for selective detection of emitted light without interference from reflected and scattered light from the excitation beam. Excitation and emission filters are selected for particular fluorophore to maximize its signal-noise ratio.

Fluorescence quantum yield (ϕ) is defined as the ratio of the number of photons emitted to the number of photons absorbed.

Another factor is the molar extinction coefficient (ε), which describes how readily a molecule absorbs light of a determined wavelength.

The product of ϕ and ε gives the brightness: the molecule's propensity both to absorb and to emit light (Fluorescein ϕ=0,85)[6]

Several extrinsic factors, classified as quenching, can decrease the fluorescence. Static quenching occurs when fluorophore forms aggregate[7].

Self-quenching (homotransfer) is a type of Forster resonance energy transfer that occurs when the fluorophore is at high concentration in solution or locally and the energy of S1 is transferred to another fluorophore rather than emitted as fluorescence[8].

A related phenomenon is the inner filter effect, which starts at lower concentrations, where emitted light is absorbed by fluorophore directly in its path[2]. Fluorophores can also be coupled to quenchers via a linker that breaks when exposed to low pH[9] or tumor specific enzymes[10]. Once the fluorophore and the quencher are separated the quenching effect is eliminated and fluorescence is restored. Quenching may affect the imaging in tumor tracer avid.

Photobleaching is the degradation of the fluorophores upon irradiation with light. Excited fluorophores react with other molecules to generate non-fluorescent products[11]. The rate of photobleaching depends on the chemical reactivity of the dye and the intensity of excitation light. Photostability is related to the fluorescent quantum yield because non-radiative pathways are often involved such as intersystem crossing. In practice, during surgery this phenomenon may be delayed by the

presence of surgical instruments, cotton pads or tissue but it may become a problem if the tumor is exposed to light too long[2].

Auto-fluorescence arises from the natural fluorescence of human tissue due to endogenous amino acids, enzyme co-factors and hemoglobin. This phenomenon is greatest at shorter wavelength (300-550nm) [12].

Fluorescein

Fluorescein is a well-tolerated yellow-green xanthine fluorophore first used in ophthalmic angiography, then for cerebrovascular procedures and to detect cerebrospinal fluid leaks[13,14]. Fluorescein is a passive dye and extravagates from the vasculature into tissue where the Blood Brain Barrier (BBB) is disrupted or when there is high vasculature permeability which may not be seen in all tumor types. Fluorescein accumulation is not restricted to the tumor tissue and may be found in areas of edema or surgical injury[15].

The main characteristic is its high brightness, which yields a valid signal even at lower concentrations. The Sodium fluorescein has demonstrated utility because its chemical structure provides a unique excitation and emission fluorescence spectrum. It is an organic molecule with the empirical formula $C_{20}H_{10}Na_2O_5$ [16] (Fig.2).

Chemical name: disodium 2-(3-oxo-6oxido-3H-xanthen-9-yl) benzoate.

Molecular weight (MW): 376.3

Fig. 2 Chemical formulation of Sodium Fluorescein

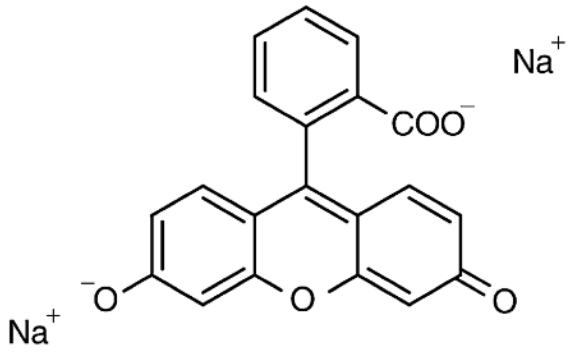

The Fluorescein acts as a nonspecific extracellular fluorophore. Its excitation peak occurs at 480 nm (range 465-490 nm) with emission peak at 525 nm (range 500-530nm) (Fig.3).

Fig. 3 Excitation and emission wavelength peaks of sodium Fluorescein.

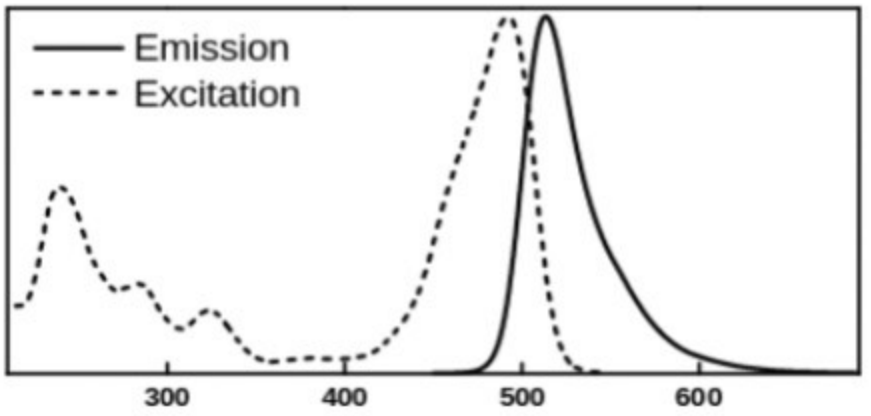

The Fluorescein passes the blood brain barrier (BBB) disrupted by the tumor. MW 376 Da; an intact BBB preclude the passage of molecules with a MW> 180 Da [17,18]

After injection Fluorescein binds to albumin in a reversible fashion (70-80%) during the first hour. About 15-17% is bound to erythrocytes. Fluorescein undergoes rapid metabolism to fluorescein monoglucuronide in a period of 1 hour post-dose. Fluorescein monoglucuronide is about 1/3 to ¼ as fluorescent as fluorescein, depending on the wavelength of excitation of the blue light. Fluorescein and its metabolites are mainly eliminated via renal excretion. After intravenous administration, the urine remains slightly fluorescent for 24 to 36 hours.

Mechanism of the Fluorescein

The BBB consists of a confluent layer of highly specialized microvascular endothelial cells covering capillaries intertwined by astrocytic processes forming tight junctions (TJs) in the brain. Brain capillaries are shielded by mature pericytes sharing the basement membrane with the endothelium, which together with astrocytes secrete basement membrane matrix proteins. While BBB is fairly permeable to small molecules and lipid-soluble proteins, larger molecules require receptor-mediated transcytosis to enter the Central Nervous System (CNS)[19]. The endothelial cells comprising most CNS blood vessels lack fenestration and have diminished pinocytosis. They are connected by tight junctions which consist of occludin and

claudins, which link to the cytoskeleton through scaffolding proteins (Zonula occludens-ZO-1,ZO-2,ZO-3 and cingulin). Adherents junctions, including cadherin, link endothelial cells and connect to actina filaments through alpha, beta e gamma catenins. The matrix components of the basal lamina (laminins, proteoglycans, fibronectin, type IV collagen) play an important role in the regulation of BBB and contribute to the interaction between endothelial cells and astrocyte endfeet. Astrocyte endfeet form the glia limitans, which covers the entire surface of the brain and spinal cord and separates the perivascular space from the brain parenchyma. Molecules from 0.8 to 70 kDa have been shown to penetrate the glia limitans to a varying degree; whereas molecules from 150 to 2000kDa are confined into the perivascular space. The 20nm gaps between astrocytes endfeet are likely to generate a crucial cutoff for diffusion of molecules into interstitial fluid. The glia limitans and basement membranes create a barrier between circulating components of immune system and CNS parenchyma; this is integral in the neuroimmune axis. The close proximity of astrocytes endfeet and endothelial cell has led to the fact that glia limitans can affect BBB permeability[20].

Within the meninges, blood vessels differ based on their anatomical location. Endothelial cells in the dura mater lack tight junctions and allow extravasation of molecules as large as 43 kDa. At the level of choroid plexus, the endothelium is fenestrated and lack tight junctions and glia limitans; however ependymal cells overlying these vessels have tight junctions and form a blood-cerebrospinalfluid barrier composed of transmembrane proteins. Similar to the choroid plexus, circumventricular endothelium and lack tight junctions and lamina

terminalis. Like choroid plexus, the circumventricular organs has highly specialized ependymal cells called Tanycytesand form a barrier. Tanycytes are connected with tight junctions that include ZO-1, occluding.claudin-5 and claudin-1, which limits diffusion of macromolecules [20,21].

Because astrocytes maintain the anatomical and physiological function of BBB, disease affecting astrocytes can affect the BBB. Water transport across the BBB is mediated by aquaporin 4, expressed along astrocyte endfeet and controls flow of ions, macromolecules and fluids. The endothelial lining of the neurovascular unit also possesses a multitude of transport protein (p-glycoprotein, MRP transporters,…). They mediate efflux of xenobiotics from the endothelium or into the endothelium away from the intraparenchymal fluid compartment.

The presence of malignant tumors results in alteration and disruption of BBB. Pathological vascular changes within the tumor can be attributed to the astrocytic diffuse upregulation and redistribution of aquaporin 4, decreased claudin and occluding expression within the TJs, basement membrane disruption and leaky neovascularization. These lead to an increase of permeability at the blood-tumor barrier facilitating influx of proteins and inflammatory mediators into the brain parenchyma [21]. Vascular damage during brain injury or tumors is a type of sterile injury; it triggers a rapid inflammatory response with activation of cytokine, chemokine and recruitment of peripheral myelomonicytic cells [20].

Associated to vascular changes, hypoxia and acidotic microenvironmental conditions contribute in increasing blood tumor barrier permeability through induction of hypoxia inducible factor 1 (HIF1). Induced production of vascular endothelial growth factor (VEGF) contributes directly to hypoxia via angiogenic tortuous and leaky vasculature with gaps in the basement membrane and endothelium.

Tumor vessels of highly angiogenic lesion are both enlarged, thin-walled, tortuous and hyperplastic vessels. These fast-growing vessels have premature endothelial cells with leaky BBB tight junction resulting in high permeability. This results in a vasogenic edema that causes further disruption of the tight junctions. Moreover this edema causes osmotic shrinkage of the brain capillary endothelial cells. All these facts lead to an increased BBB permeability and to an early extravasation of the Fluorescein into the tumor interstitial space [15,21,22].

This mechanism is similar to the accumulation of Gadolinium used as a contrast agent in MRI. Thus we found a correlation with Gadolinium enhancement and the intensity of Fluorescein. In fact, in cases of homogenous and high hyperintensity after Gadolinium administration, the lesion has a high fluorescein intensity. We can postulate, at this moment only from an optical point of view, that the fluorescein intensity which we will find intraoperatively is proportional to the Gadolinium enhancement Intensity on Magnetic Resonance Imaging (MRI)[23].

In the work of Neira et al., during GBMs surgery and biopsy, there was found correlation between fluorescein intensity and contrast

enhancing regions, and non-contrast enhancing regions. They found intense fluorescein staining in both contrast and non-contrast enhancing regions as localized by preoperative MRI because of the differential permeability profiles of fluorescein and gadolinium[23] .

Folaron et al. described the kinetics of fluorescein; upon administration, Na-Fl binds to blood proteins, resulting in a mixture of bound/unbound Na-Fl to endogenous proteins. The 376 D unbound Na-Fl penetrates the normal brain tissue, readily crossing the BBB, while the bound dye (66kD) remains in the circulation. Fluorescein distribution is initially heterogeneous, with highest concentration near the ventricles, probably due to leakage from the CSF barrier, which is known to be more permeable than BBB; yet it decreases and becomes more uniform over time. The concentration of unbound/ bound Na-Fl in the blood depends on the injecting dose and elapsed time from injection. The fluorescein signal in normal brain tissue arising from unbound Na-Fl is time-dependent, peaking between 15 and 30 minutes after injection and decreasing thereafter. So, during clinical use of fluorescein, the administration to resection intervals varied from immediate to hours; at longer intervals, the Na-Fl in the normal brain is well below the peak levels, therefore the signal present is the extravasation of the dye in damaged BBB. They also described the kinetics of Pegylated-fluorescein (size similar to Gadolinium), that did not dissociate in the blood and has a low uptake in the normal brain even at early time of injection. This formulation was suggestive in providing improved tumor delineation because of its accumulation in regions where the BBB was disrupted by tumors[24].

In other studies, authors used Na-Fl conjugated to serum albumin and tested during surgery. Their reports indicate that the human serum albumin-NaFl molecules dissociate in blood circulation resulting in the presence of unbound Na-Fl in tumor samples[25].

The other mechanism of the Na-Fl is the overexpression of membrane transporter such as MRP1 (multi drug resistance associate proteins) on tumoral cells, of which Na-Fl is a substrate. This is an efflux anion transporter, that contributes to concentrate the Fluorescein in the tumoral cellular matrix[26].

For peripheral lesion, this dye accumulates in high vascularity lesion, such as schwannomas and inflammatory lesions, and also in neoplastic lesions with abnormal blood vessels.
Peripheral nerves are structurally organized in 3 compartments: the outermost epineurium through which extrinsic blood vessels (vasa nervorum) penetrate to give rise to epineurial arteries and arterioles and receive blood from epineurial venules and veins, the inner perineurium, formed by epithelioid myofibroblast form fascicles and the innermost endoneurium, which consists of myelinated and undmyelinated axons. Ultrastructural examination has demonstrated that endoneurional microvessels and the innermost layers of perineurium form electron-dense intercellular tight junction; epineurial arteries, arterioles, venules and veins (known as macrovessels) are fenestrated. Endoneurial microvessels are in direct communication with circulating blood and are considered the Blood-Nerve Barrier (BNB), while the perineurium restricts passive diffusion of interstitial

fluid from the epineurium into the endoneurium and vice versa. The BNB serves to maintain the internal endoneurial microenvironment essential for physiological signal transduction by axons to and from the CNS [27,28]. As in the BBB the essential component is the TJs. TJs consist of a network of transmembrane and peripheral proteins (claudins, occludins, junctional adhesion molecules and zonula occludens) that are important for restricting the paracellular flow of ions and molecules into the endoneurial milieu. Secretion of bFGF by BNB-derived pericytes strengthens the barrier function by increasing the expression of claudin-5 [29].

One study, in 1980 by Malmgren and Olsson, showed that in rodents the diffusion characteristics of high doses of fluorescein in CNS and PNS were different: higher fluorescence level in the epineurium and perinerium lower level within nerve fascicles. They also noted that the degree of extravasation was different between different fascicles in the same nerve and in different nerves in the same animal. The accumulation within the endoneurium was the result of direct extravasation of Na-Fl from endoneural blood vessel. Small nerve branches (<100mu diameter) showed more extensive penetration of Na-Fl into the endoneurium than larger nerve branches. This might be due to a diffusion of Na-Fl along the extracellular space to the endoneurium from nerve terminals where the perineurial barrier is open-ended[30].In other experimental work, Perez at alt. showed that merlin-deficient Schwann cells and in vestibular schwannoma cells internalize much higher levels of Na-Fl and enhance significantly brighter than other cell types. They also found in vitro experiments that fluorescence intensity was also dependent on concentration of Na-Fl,

duration of treatment, cell density and total time of blue light excitation[31]. The key point in Na-Fl accumulation is the disruption of the blood-nerve barrier (BNB). It defines the blood-tissue interaction within the peripheral nerve endoneurium to maintain ionic concentration essential for physiological action potential conduction[28]. Following nerve injury, nerve edema evolves in the distal segment caused by an increase in endonuerial fluid pressure accompanied by long-lasting disruption of the BNB. At the injury site, resident macrophages have been shown to alter the permeability of microvessels and breakdown of the BNB via expression of the cytokine vascular endothelial grow factor (VEGF). Increased permeability of BNB appears to involve TJ changes and influx of molecules into the peripheral nervous system. At the level of the injury reduction of expression of ZO-1 was found in endoneurial vessels leading to a breakdown of BNB[29] as shown in previous studies in rat models[32]. Local nerve inflammation due to an externally induced nerve damage involves secretion of cytokines and chemokines by Schwann cells, which attracts leukocytes facilitating their extravasation at sites of injury. The BNB increased permeability induce microvascular abnormalities in the endoneurium (degradation of tight junctions, loss of perivascular pericytes, increased basement membrane thickness, endothelial cell hyperplasia) and a subsequent endoneurial hypoxia[29]. Tumor growth alters tight junctions, through a vascular and inflammatory network and leads to fluorescein extravasation and accumulation into neoplastic lesions.

Material and Method

21 patients (7 females, 14 males) underwent surgery in Varese with the use of Pentero 900 microscope with the yellow 560 nm dedicated filter (Karl Zeiss). 17 patients (9 females, 8 males) underwent surgery in Monza using the Spetzler lighted suction tube (Kogen Surgical) connected to the blue light (Karl Storz). Patients must preoperatively provide written informed consent.

Patients' inclusion criteria:

a) both genders

b) any age, adults and pediatrics

c) Patients with lesion of the Central Nervous system or Peripheral Nervous system enhancing on MRI with contrast.

Exclusion criteria:

a) Impossibility to give consent due to cognitive deficits or language barrier.

b) Known allergy to contrast agents and/or history of previous anaphylactic shocks.

c) Known severe previous adverse reactions to Fluorescein

d) Acute myocardial infarction or stroke in the last 90 days.

e) Severe renal failure (specific glomerular filtration rate < 60, serum Creatinine >1,2 mg/dl for women; >1,4 mg/dl for men);

f) Severe hepatic failure (high Aspartate transaminase/Alanine Transaminase ratio);

g) Women in their first trimester of pregnancy or lactation.
h) Patients who had contraindication for an MRI-scan

Precaution for drug interaction:
Angiotensin-converting enzyme inhibitors: increased risk of adverse reaction
Beta blockers: patients on beta blockers are at increased risk of adverse reaction when administered fluorescein due to an interference of beta blockers at the level of the beta-receptor; beta blocking agents could reduce the vascular compensation reactions to anaphylactic shock and reduce the effectiveness of adrenaline in the presence of cardiovascular collapse.
If fluorescein injection is deemed necessary monitor as appropriate during and after procedure.
Neuroradiology:
Patients undergo 2 main imaging: Pre-operative MRI with and without contrast, functional MRI and trattography (DTI-diffusion tensor imaging) for lesions near eloquent area.
Post-operative MRI with contrast within 72 hours or 2 months from surgery

Dose and Timing for Fluorescein injection

As confirmed by previous study, the time of injection is an important factor in allowing discrimination between tumor and healthy parenchyma. In the letter to the editor, Acerbi et al. have suggested using a low dose (5 mg/kg) of fluorescein, intravenous administrated at the end of intubation (i.e. 1 hour before dural opening). With this

timing of injection they always found good discrimination between fluorescent and non-fluorescent tissue[33]. The acute injection of NaFl is associated with an intense uptake even by normal tissue as described by Folaron, owing to the passage of the dye throughout small capillaries during normal brain perfusion[24]. This type of injection is indicated for vascular indication.

Na-Fl was approved in Italy for neuroncology, but for peripheral lesion this dye is still off-label; thus informed consent covering application of Na-Fl during surgery was obtained from all patients. The study is in accordance with the ethical principles that are reflected in the Declaration of Helsinki. Also, the study was coordinated with the ethics committee of our Institution.

Surgery

Before surgery all image-sets are uploaded in the neuronavigation system for surgical planning. Neuronavigation (Brainlab AG Olof-Palme-Straße 9, Munich Germany) is allowed only for surgical planning, initial tumor localization and orientation during tumor removal, but not for judgment regarding extent of resection.

At the induction of anesthesia (or at least 30 minutes before tumor exposure), patients receive 5 mg/kg (3mg/kg in the pediatric population) of intra venous sodium fluorescein-Monico Spa, Italy- (22 July 2015, Gazette n.168, determination 905/2015: AIFA Approval in neuroncology) (Fig.4).

Fig. 4 Sodium Fluorescein vial, Monico Spa, Italy

Surgery is performed by using a dedicated surgical microscope; the Pentero 900 with fluorescence YELLOW 560nm filter (Karl Zeiss) or with the Spetzler lighted suction tube (Kogent surgical) connected to the blue filter at 490 nm from Karl Storz with yellow filter at 560 nm adapted to the surgical microscope cover (Fig.5 A,B,C). No heat was detected at the light suction tube, even after longer surgery.

Fig. 5 Device used in Monza for fluorescein guided surgery.

Fig. 5 A. Blue light filter connected to the light source (Karl Storz-Germany)

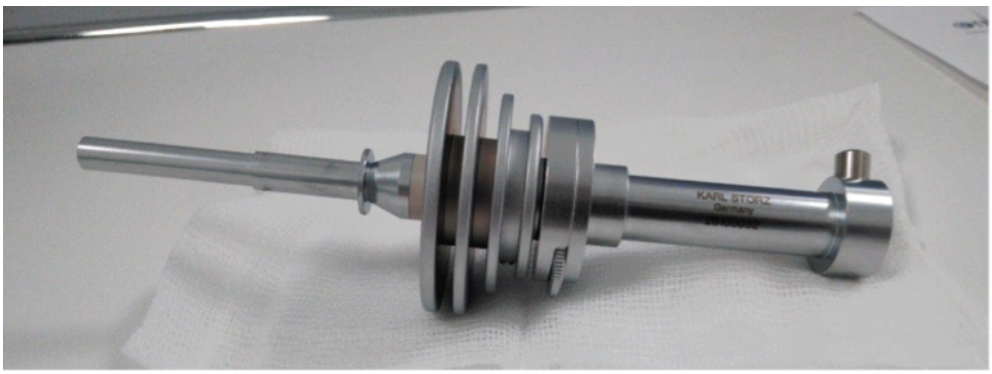

Fig. 5 B On the left side yellow filter at 560 nm, on the right side the Spetzler lighted suction tube (Kogent Surgical)

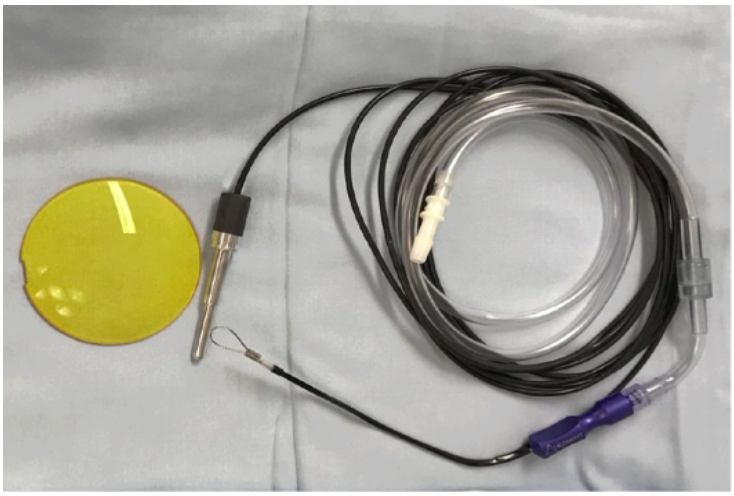

Fig.5 C lighted suction tube with the blue light.

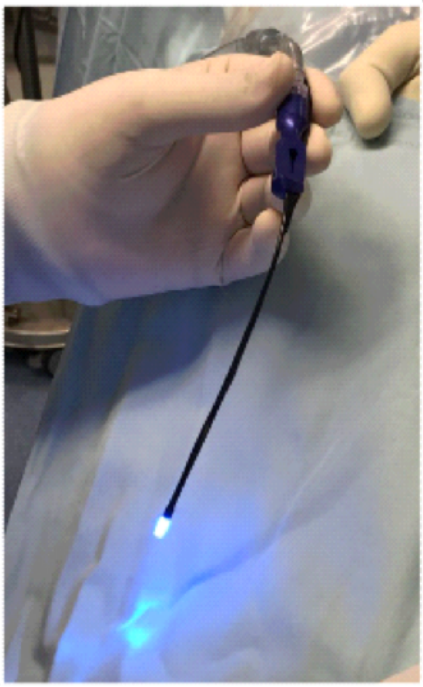

Surgical removal is performed with a standard microsurgical technique by using both white light and yellow light illumination in alternating fashion.

The surgical technique for resecting extra-axial lesions such as brain metastases or meningiomas is different from that of removing gliomas. Metastases and meningiomas are delineated from healthy parenchyma and can be removed en bloc followed by circumferential dissection of the residual tumor capsule. In contrast gliomas have an irregular brain-tumor interface so they are removed by piecemeal technique.

During surgery we used neuronavigation to check enhancing lesion to residual fluorescence (Fig. 6 A,B).

Fig. 6. correspondence between intraoperative neuronavigation and residual fluorescence at the end of surgery.

A. neuronavigation imaging showing the pointer in a contrast enhancing region.

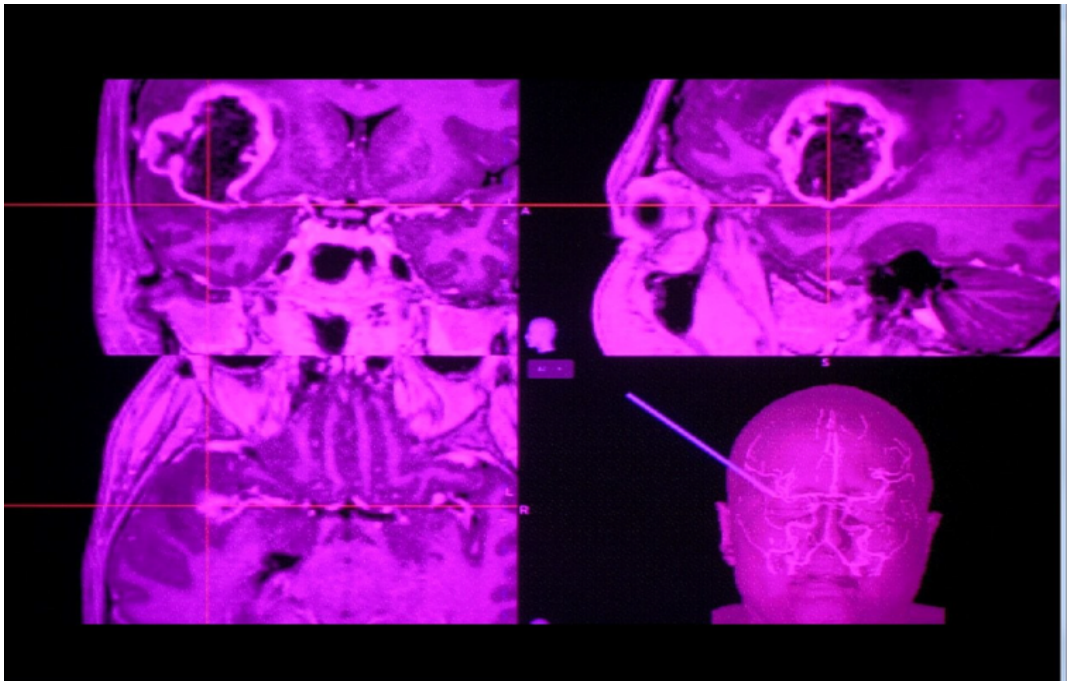

B. residual fluorescence in the surgical cavity corresponding to the pointer level.

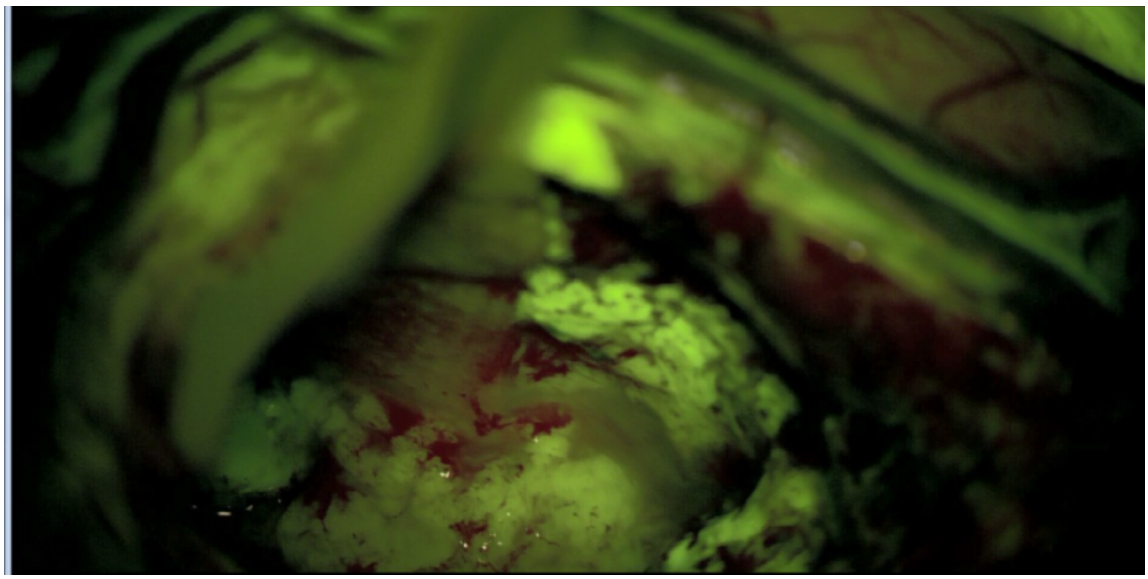

Our protocol for lesions in eloquent area and peripheral nerve surgery consisted in all cases of intraoperative monitoring to identify the safest entry point in the cerebral parenchima and inside the pseudocapsule of schwannomas, and to verify, during and at the end of the procedure, the functional integrity of the healthy tissue.

Fluorescence intensity measurements in region of interest (tumor areas, margins and normal/healthy parenchima, dura) are processed using Image J software (Version 1.53a, Wayne Rasband, National Institute of Health, USA) and a comparison is made between the red, green and blue emission channels of the different tissue in the different areas. Secondly we correlate the Fluorescein intensity with the histology of the tissue. The control regions are the dura for the

fluorescent tissue and the healthy parenchima, far away from the pathological tissue, for the non-fluorescent tissue (Fig.7).

Fig. 7 Image J study in RGB scale. 1. dura (191,255,60); 2 lesion (204,255,60); 3. margin (120, 133, 136); 4. healthy parenchyma (104,90,34)

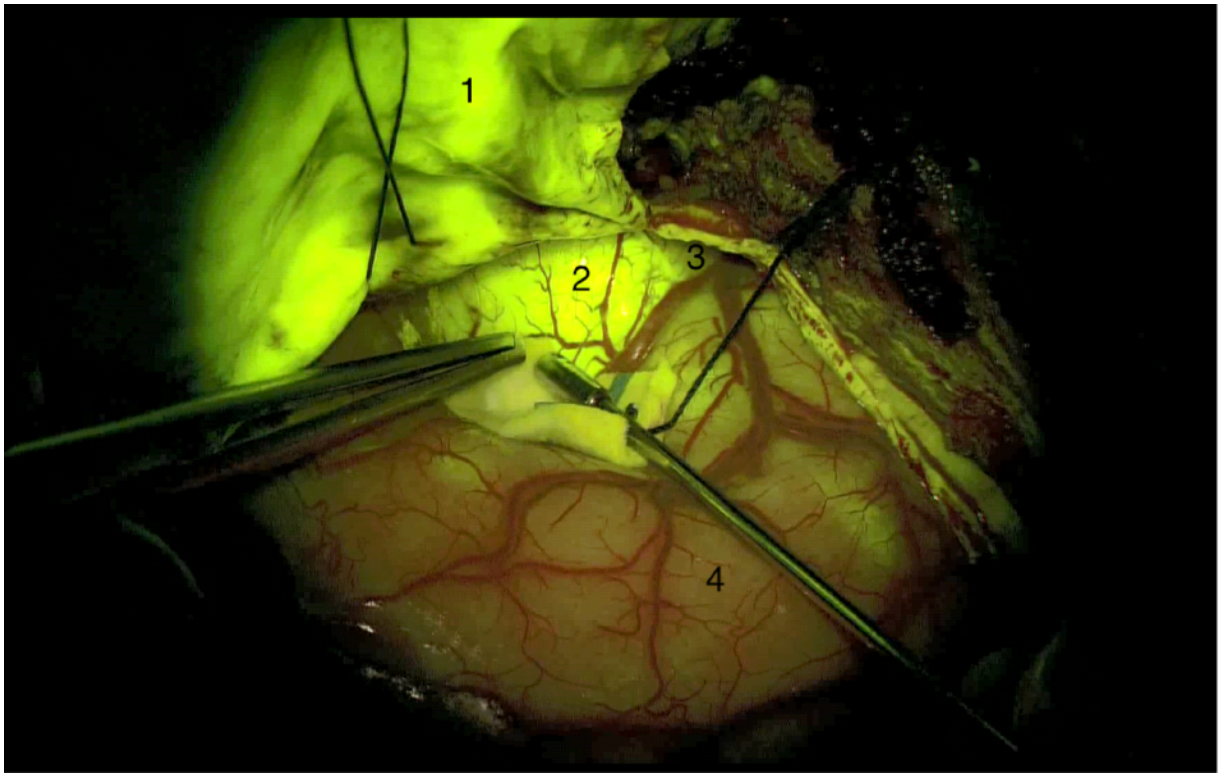

For statistical analysis we used Excel Microsoft Office Software (2019). RGB acquired data were expressed by mean value, maximum value, minimum value and standard deviation.

Results

In our study we have used fluorescein in intracranial and peripheral lesion, despite the histology. This, to have a wide experience with this dye and to know the utility of the Na-Fl in different pathologies.

In Varese we performed cranial surgery in 21 patients, between 16 and 77 years old. Mean age 50,76 years old. The histology of the lesion was Glioblastoma (WHO grade IV) in 11 cases, 1 anaplastic glioma (WHO grade III), 2 ependymomas (WHO grade II), 2 pilocityc astrocytoma (WHO grade II), 1 meningioma (WHO grade I), 2 atypical neurocytoma (WHO grade III), 2 metastasis. Table 1 shows the characteristics of the study population in Varese.

Table 1: study population in Varese. The table shows age, sex, histology, NaFl dose, Infusion time and side effects. GBM Glioblastoma

Pz	Age	sex	Lesion Localization	Histology	NaFl dosage	Timing injection	Side effect
1	50	M	Left frontal	GBM	5 mg/kg	Anestesia induction	none
2	69	M	Left temporal	GBM	5 mg/kg	Anestesia induction	none
3	54	F	cerebellar	Lung metastases	5 mg/kg	Anestesia induction	none
4	16	M	Right frontotemporal	Anaplastic glioma	5 mg/kg	Anestesia induction	none
5	51	F	Left temporoparietal	Meningioma	5 mg/kg	Anestesia induction	none
6	53	F	cerebellum	Breast Metastases	5 mg/kg	Anestesia induction	none
7	41	F	sovrasellar	GBM	5 mg/kg	Anestesia induction	none
8	55	M	Right temporal	GBM	5 mg/kg	Anestesia induction	none
9	34	M	cerebellar	Pilocytic Asrtocytoma	5 mg/kg	Anestesia induction	none
10	54	F	Left Paratrigonal	GBM	5 mg/kg	Anestesia induction	none
11	30	M	Right lateral ventricle	neurocytoma	5 mg/kg	Anestesia induction	none
12	69	M	Left frontoparietal	GBM	5 mg/kg	Anestesia induction	none
13	61	M	Right frontal	GBM	5 mg/kg	Anestesia induction	none
14	77	F	Right Temporo occipital	GBM	5 mg/kg	Anestesia induction	none
15	28	M	Right temporoparietal	GBM	5 mg/kg	Anestesia induction	none
16	68	M	Right temporal	GBM	5 mg/kg	Anestesia induction	none
17	58	M	IV ventricle floor	ependymoma	5 mg/kg	Anestesia induction	none
18	35	M	Right cerebellar	Pilocytic Astrocytoma	5 mg/kg	Anestesia induction	none
19	53	F	Right frontal	GBM	5 mg/kg	Anestesia induction	none
20	50	M	IV ventricle	ependymoma	5 mg/kg	Anestesia induction	none
21	60	m	Left temporal	neurocytoma	5 mg/kg	Anestesia induction	none

As shown in table 2, in Monza we performed surgery in 17 patients, between 23 and 75 y.o; mean age 55,53 y.o. The histological diagnosis is 3 glioblastoma (WHO grade IV), 2 meningiomas (WHO grade I), 2 acustic schwannoma, 1 oligoastrocytoma (WHO grade III),

2 spinal schwannoma, 2 ependymomas (WHO grade II), 4 peripheral schwannomas, 1 corpora Amylacea.

Table 2: study population in Monza. The table shows age, sex, histology, NaFl dose, Infusion time and side effects. GBM Glioblastoma.

Pz	Age	sex	Lesion Localization	Histology	NaFl dosage	Timing of infusion	Side effect
1	61	f	L3 Spinal nerve	schwannoma	5 mg/kg	Anestesia induction	none
2	59	f	Right Sciatic nerve	schwannoma	5 mg/kg	Anestesia induction	none
3	61	m	cauda	schwannoma	5 mg/kg	Anestesia induction	none
4	61	m	Left temporal	GBM	5 mg/kg	Anestesia induction	none
5	23	m	Right ulnar	schwannoma	5 mg/kg	Anestesia induction	none
6	50	f	VIII c.n.right	schwannoma	5 mg/kg	Anestesia induction	none
7	56	m	Left frotal	meningioma	5 mg/kg	Anestesia induction	hypertension
8	75	m	Right Temporoparietal	GBM	5 mg/kg	Anestesia induction	none
9	42	f	Left Frontotemporal	Meningioma	5 mg/kg	Anestesia induction	hypertension
10	71	f	Left Frontotemporal	oligoastrocytoma	5 mg/kg	Anestesia induction	none
11	58	f	Right ulnar	schwannoma	5 mg/kg	Anestesia induction	none
12	71	m	VIII c.n.right	schwannoma	5 mg/kg	Anestesia induction	none
13	50	m	cauda	ependymoma	5 mg/kg	Anestesia induction	none
14	51	m	Left frontal	GBM	5 mg/kg	Anestesia induction	none
15	56	f	Right Axillary nerve	schwannoma	5 mg/kg	Anestesia induction	none
16	26	f	cauda	ependymoma	5 mg/kg	Anestesia induction	none
17	73	f	Right temporal	Corpora amylacea	5 mg/kg	Anestesia induction	none

We elaborated intraoperative video of 38 patients to quantify the fluorescein's intensity. From each video we obtained a screenshot from the initial, middle and end stages of surgery. We elaborated 311 images. In every image we evaluated the fluorescein intensity in 3 different sites: intralesional, peripheral and normal parenchyma. Our region of interest (ROI) was punctiform. When possible we evaluated

as a fluorescent control the RGB value of the dura mater. We used Image J software and the fluorescein intensity was calculated with RGB scale (Tab.3).

Table 3. Maximum and minimum values in RGB scale for the different histologies.

histology	Rmin	Rmax	Gmin	Gmax	Bmin	Bmax
GBM	156,0943	186,5283	197,8679	230,8679	29,18868	59,37736
schwannoma	113,5882	187,5294	126.6667	216,1765	106,9412	211,2353
Pilocytic astrocytoma	178,7273	199,0909	233,0909	244,8182	28	44,45
Pilocytic cyst	163	185	221	255	28	54
Anaplstic glioma	122,75	128,75	156,5	163	25,5	32
Oligoastrocytoma	241	251	242	254	233	244
Neurocytoma	219,5	230,3333	255	252,8333	16,83333	25,66667
ependymomas	192	249,3333	144.6667	230	114,6667	222,6667
Corpora amylacea	161,3333	190	143,6667	190,6667	110,6667	159,6667
meningioma	158,8	205,5	182	215,4	39,5	98,8
metastases	129,8	148,2	189	208,6	1,4	13,2

The mean value in fluorescent sites for the green value is 183; this mean includes intralesional fluorescence and margin fluorescence.

We extrapolated a maximum value of 255, the minimum is 68. In the red channel the mean is 148.594, the maximum value is 255 and the minimum value is 6. In the blue channel the mean value is 30.802; the maximum value is 255 and the minimum 3.

The dura mater, which is always fluorescent, has a maximum value of G that ranges between 255 and 212. R between 250 and 112, B between 149 and 0.

In the control area, the healthy tissue, where no fluorescence is found, the mean value calculated in the green channel is 74. The maximum value is 158, the minimum 4. In the red channel the mean value is 92. The maximum is 255 and the minimum 0. In the blue channel the mean value calculated is 45. The maximum value 255 and the minimum 0.

Owing to previous studies, everyone knows that Fluorescein intensity is dependent on the dosage, timing of infusion, depth of surgical cavity, zooming of the microscope and sometimes on the shadowing of surgical instruments. In our experience, we injected the same dose of 5mg/kg at induction of anesthesia. We reached the lesion in about 45/60 minutes after infusion with relevant fluorescein staining at the lesion level. We had no need of a second infusion of Na-Fl in all cases. We extrapolated RGB data from images with similar range of microscope zooming. Even though we found difference in lesion depth, the G values were not affected. We excluded high magnification images because of their less fluorescein brightness.

A limit of our study is the fact that images evaluated were not at the same magnification, so in our future work we are going to study pixel intensity of Na-Fl in images at the same microscopic magnification to maintain the same illumination.

Histopathological analysis was performed in each case and tumors were classified according to the 2016 WHO classification by the Pathology group of each Institution.

In table 4 there is the fluorescein intensity classification from the surgeon's point of view (tab.4).

Table 4. Characteristic and intensity of Fluorescein uptake: comparison between different histologies

Histology	**characteristic**	**intensity**
GBM	inhomogeneous	Moderate/intense
Anaplastic glioma	inhomogeneous	Moderate/intense spot
metastases	inhomogeneous	intense
Oligoastrocytoma	inhomogeneous	Moderate/intense spot
Pilocytic astrocytoma	Inhomogeneous	Moderate/intense spot
Pilocytic cyst	homogemeous	intense
Neurocytoma	homogeneous	intense
ependymomas	homogeneous	Moderate/intense
Corpora amylacea	homogeneous	moderate
meningioma	homogeneous	intense
schwannoma	homogeneous	moderate

In figure 8 A, B and C is shown the distribution of RGB values in fluorescent pathological tissue.

Fig. 8 A. Maximum R values found related to tissue histology

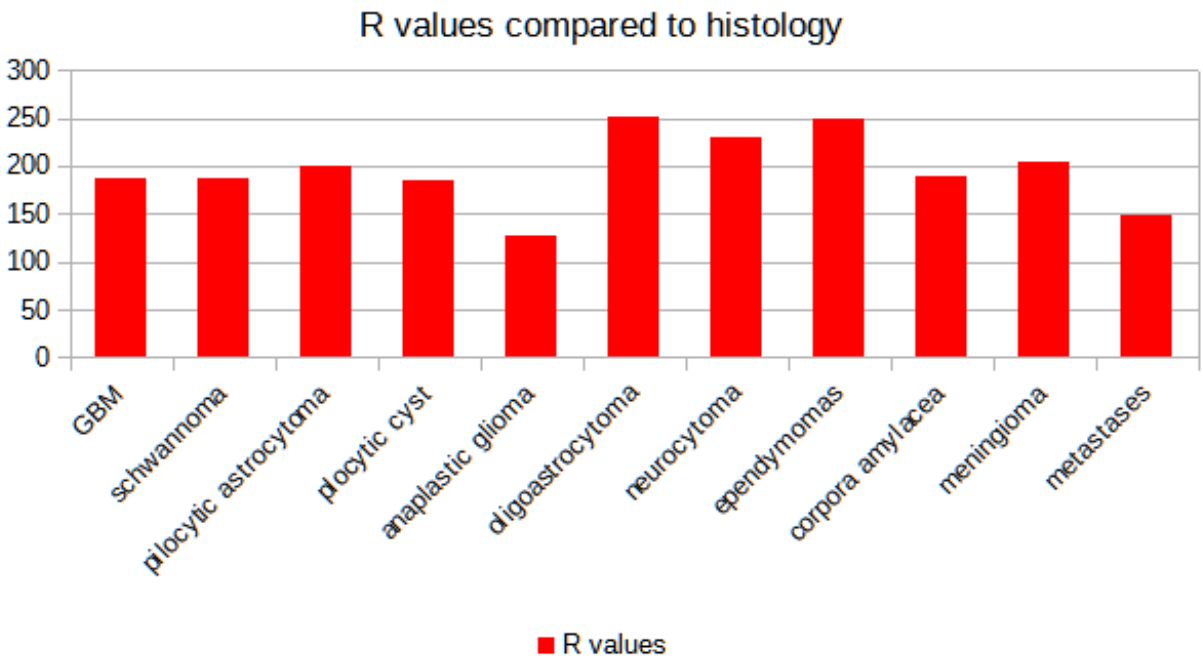

Fig. 8 B. Maximum G values found related to tissue histology

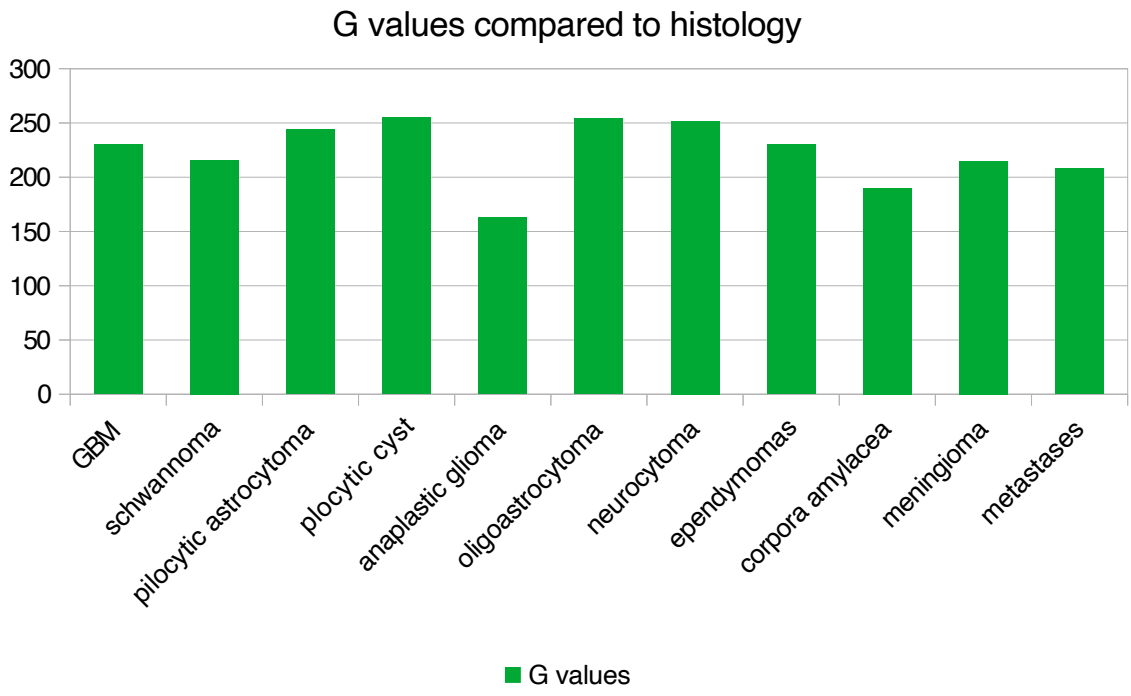

Fig. 8 C. Maximum B values found in the different histological tissue. As shown in the graph, the B values are the less significant.

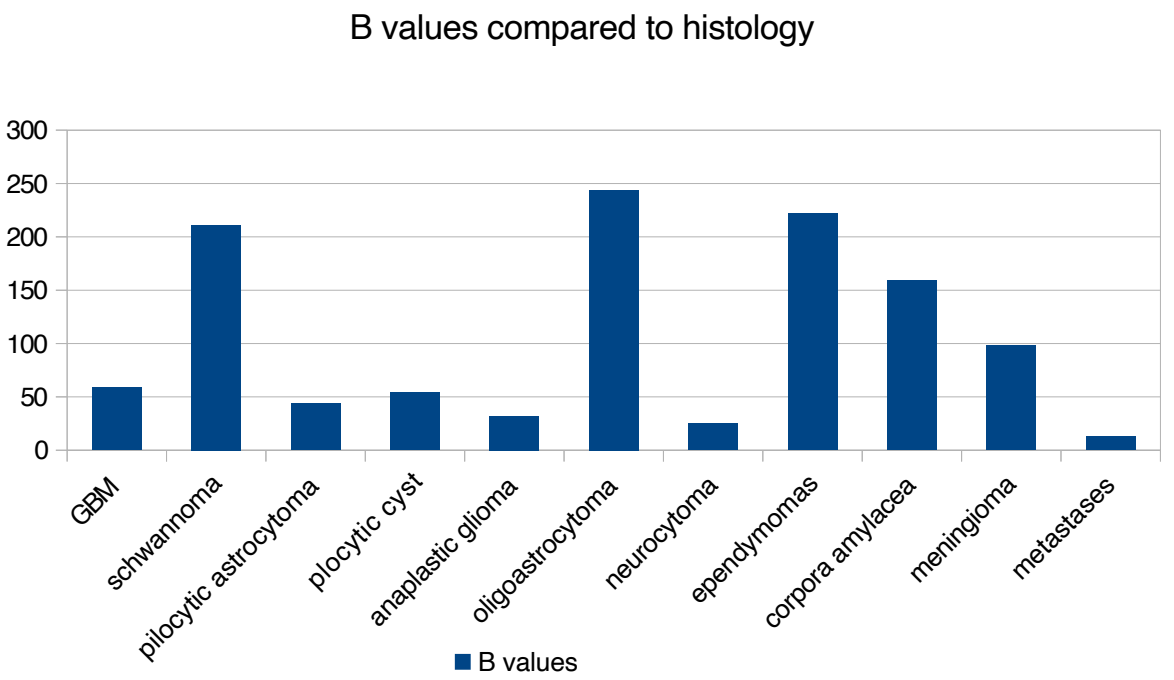

In our study we noticed that High-grade glioma usually presented bright fluorescence with a yellow-green signal clearly distinguishable by peritumoral parenchyma. The intensity of fluorescence ranged between mean value of G from 197and 230 (max 255, min 134). Sometimes, in the central necrotic core, the tissue showed a dark pinkish feature with less fluorescein uptake. This particular appearance was more pronounced in recurrent tumors and in patients already submitted to radiotherapy. Sometimes a bright fluorescent fluid component was reported as the result of tumor cells colliquation.

The same pattern was showed in metastases, which had the similar fluorescence intensity mean value of G ranging between 189 and 208 (max 250, min 179), with an inhomogeneous appearance. In WHO grade I and II we found few brightly fluorescent spots. In pilocytic astrocytoma was found a bright nodule with fluorescent peripheral cyst. The fluorescein enhancement was intense in the solid nodule, with mean G values ranging from 233 and 244 (mx 255, min 175) and the fluorescent intracystic fluid had an intense mean value of G from 221 to 255 (Fig.9).

Fig. 9 Fluorescence at the opening of cyst in a pilocytic astrocytoma

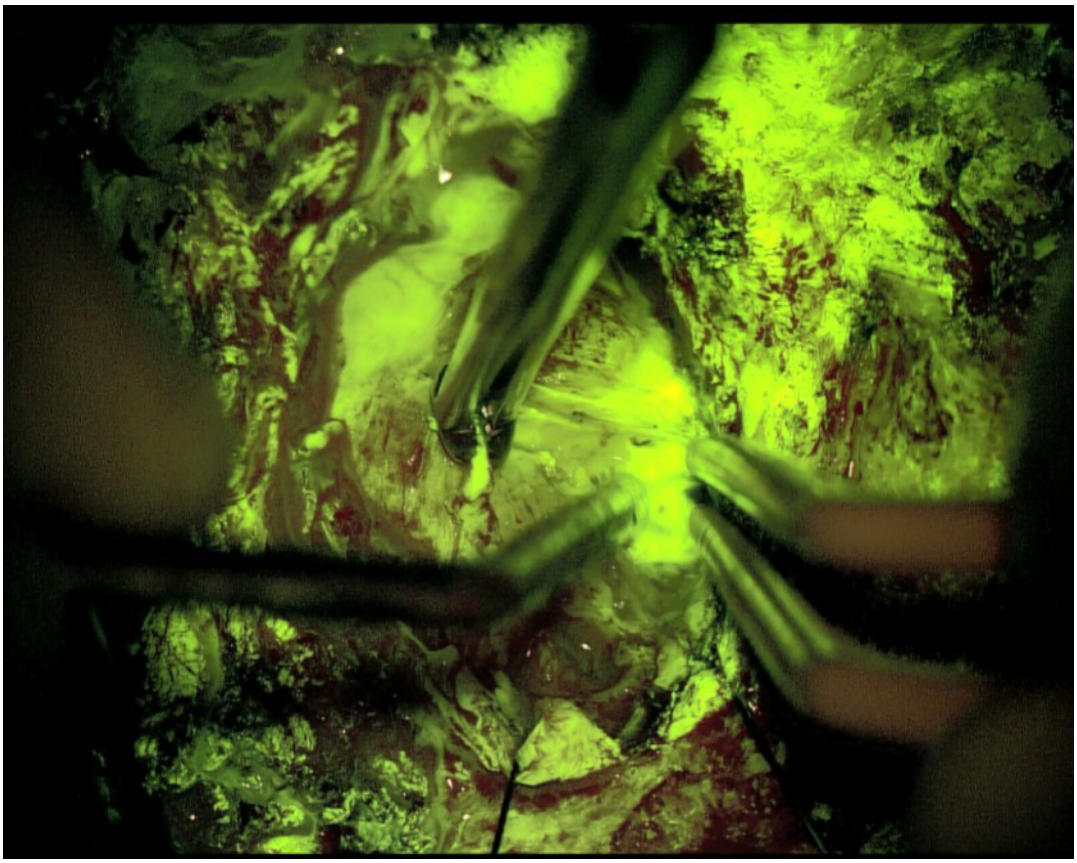

As Pilocytic nodule, similar values were found in WHO grade III lesion (mean G between 242 and 254, max 255, min 221). In meningioma we found a bright and homogeneous intensity of fluorescence. The mean values in G were similar to the high grade glioma.(182-215, max 255, min 137). Ependymomas had an intense fluorescence. The mean values ranged between 144 to 230 (max 243, min 113). Neurocytomas had intense and homogeneous fluorescent enhancement. The mean values of G were from 252 to 255 (max 255, min 242). Peripheral, spinal neurinoma and VIII cranial nerve schwannomas showed a bright and homogeneous intensity pattern of fluorescence with a mean intensity of G from 126 to 216 (max 255, min 103). In the singular case of corpora amylacea, the aspect of fluorescence was homogeneous and moderate. The mean G value was between 143 and 190 (max 248, min 113).

For statistical analysis, Excel (Microsoft Office 2019) software was used. After testing normal distribution, standard deviation (tab.5) and P value (tab.6), $P<0,05$ was determined as statistically significant. Data elaboration revealed significant ($P_{green} = 0,004$) values for the color green in histological significant tissue. The other colors, red and blue, did not reach statistically significant values ($P_{red}=0,09$; $P_{blue}=8,2$) (Fig.10). From the box-plot diagram for G values we extrapolated the threshold of 167 (first quartile) in affected patients. In the same graph we extrapolated the median value of 220 (Fig.11 A,B,C).

Tab.5 mean values and standard deviation for pathological tissue and healthy parenchyma.

	Mean +/- SD in affected	Mean +/- SD in healthy
Red	176,86 +/- 46,9	92,977 +/- 47,557
Green	207,82 +/- 44,42	75,081 +/- 27,008
Blue	65,19 +/- 71,18	47,056 +/- 44,338

Tab.6 P values in affected and healthy parenchyma

	P value Affected	P value Healthy
Red	0,09	0,05
Green	0,004	0,99
Blue	8,2	2,2

Fig. 10. Distribution of G values in fluorescent tissue.

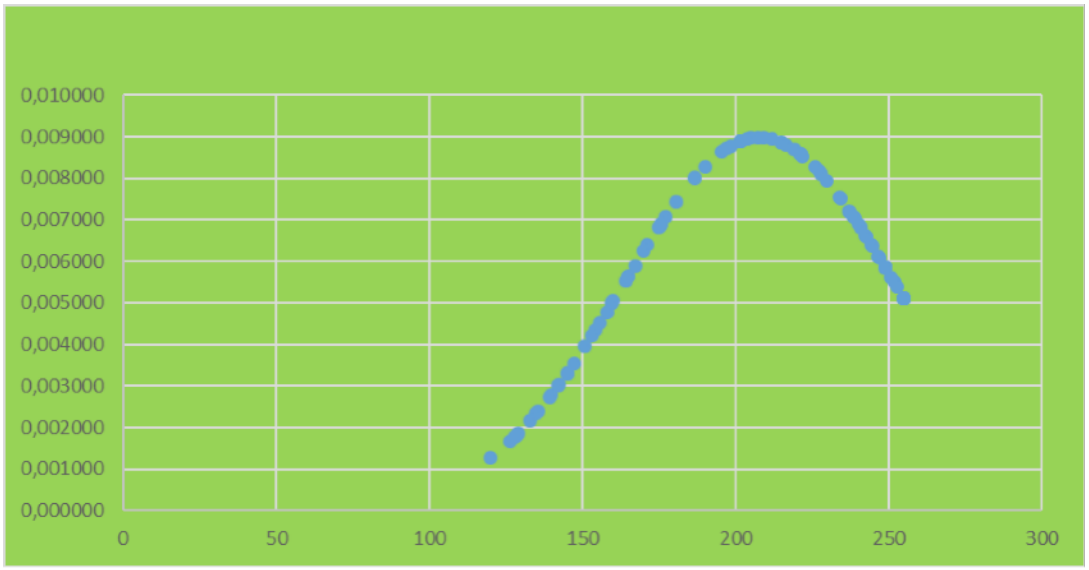

Fig. 11 A. Plotting of R values for affected/fluorescent tissue and healthy/non fluorescent tissue. Fluorescent tissue show high R values but not statistically significant.

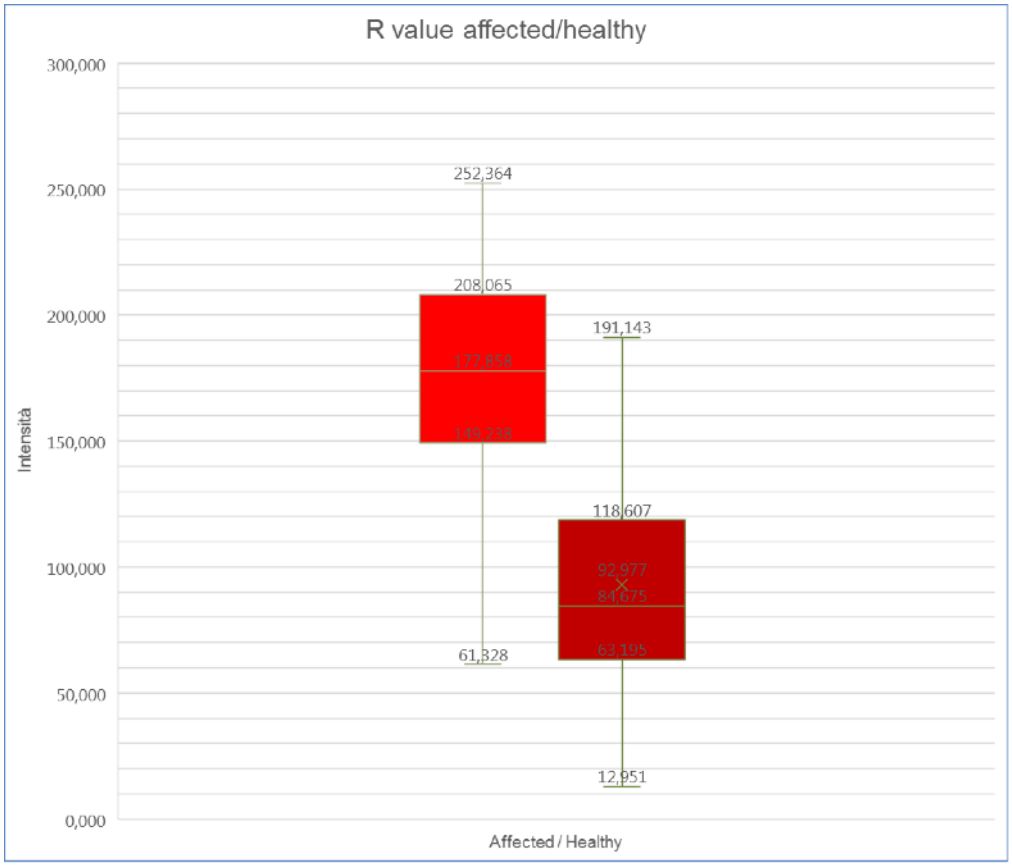

Fig. 11 B. Plotting of G values for affected/fluorescent tissue and healthy/non fluorescent tissue. Fluorescent tissue show high G values statistically significant. And 167 (first quartile) is our threshold for pathological tissue. 220 median value. 252 third quartile.

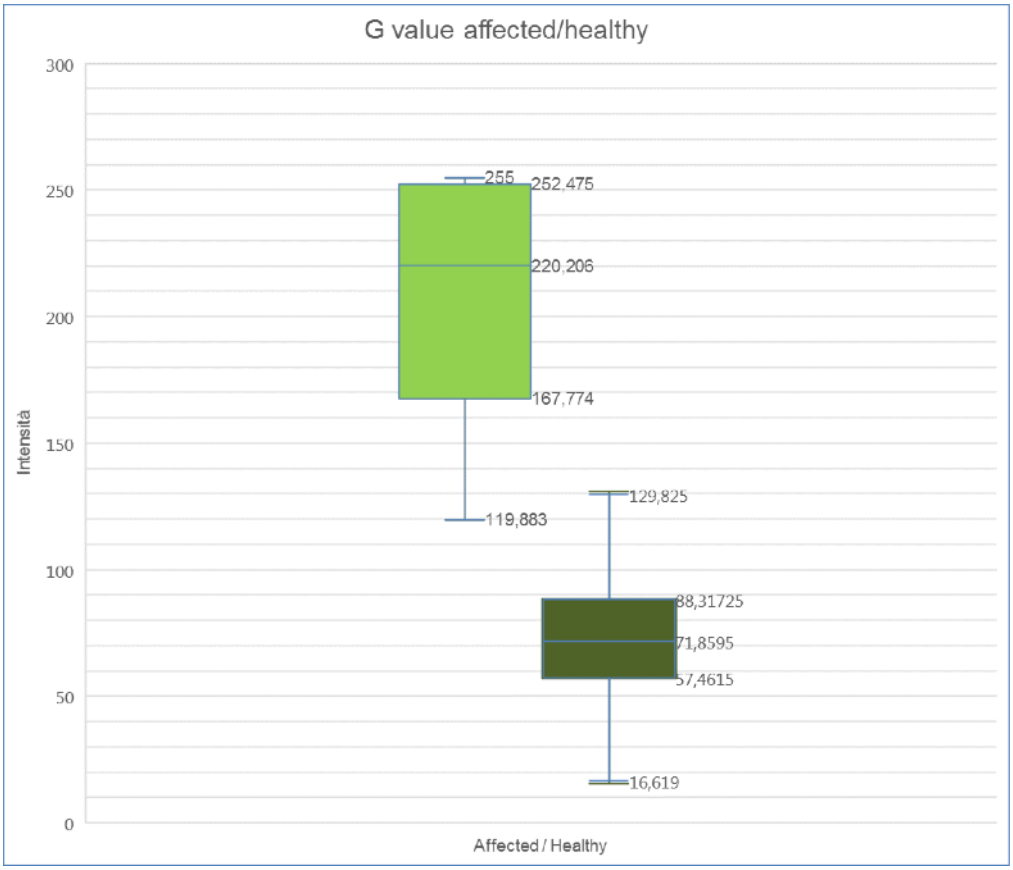

Fig.11 C. Plotting of B values for affected/fluorescent tissue and healthy/non fluorescent tissue. Fluorescent tissue shows low B values. Not statistically significant.

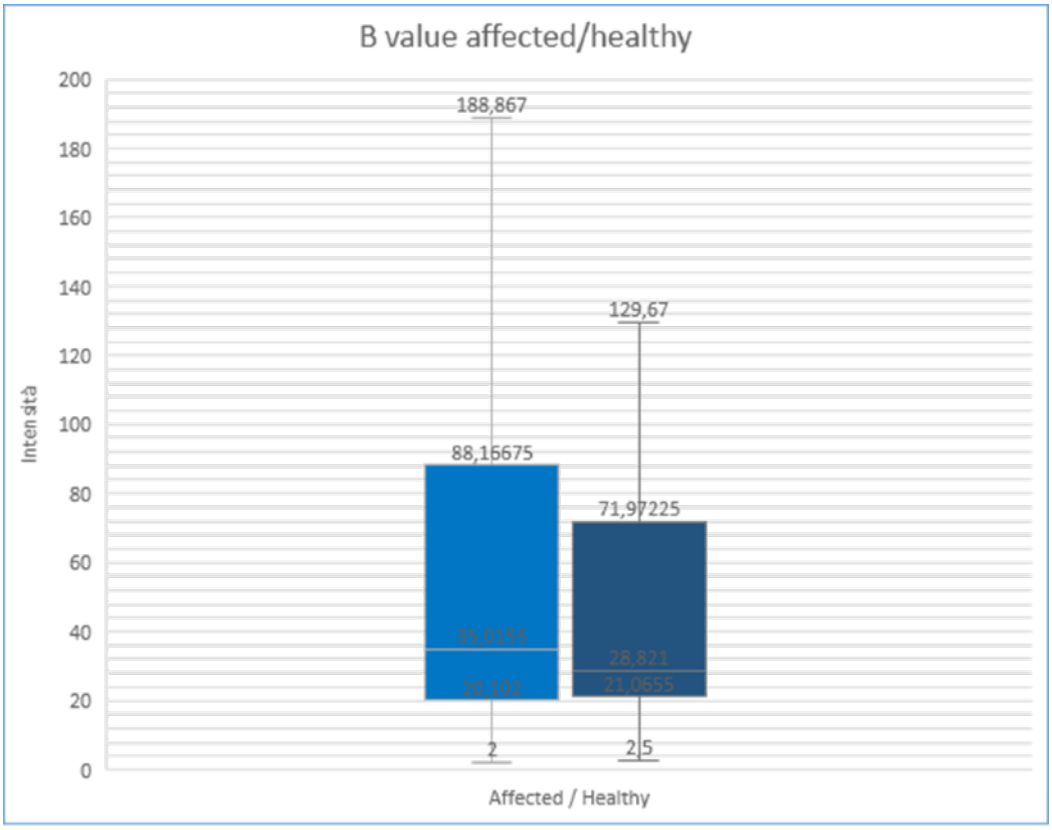

From our statistical study we can postulate that the G value is a good marker for fluorescein uptake in the lesion, and therefore a good marker for pathological tissue.

Complications

2 patients suffered from hypertension about 2 minutes after injection, which was corrected with pharmacological therapy. No alteration of heart rate was found. One patient reached a blood pressure of 180/100 mmHg treated with Trinitrate infusion. The second patient raised the blood pressure up to 150/85 mmHg and was efficaciously treated with endovenous infusion of Furosemide 20 mg and Mannitolo 125 ml. No other problems arose during surgery or the post-operative period.

In all patients, immediate but transient yellow discoloration of the skin and the urine was reported, for a maximum of 24 hours.

Table 7 offers a summary of the known side effects of Na-Fl.

Tab. 7.Side effect of Na-Fl found in the leaflet.

Very Common May affect more than 1 in 10 people	- Nausea
Common May affect up to 1 in 10 people	- Vomiting - Syncope - Redness and itching of the skin - Discolouration (yellowing) of the skin and eyes - Discolouration (yellowing) of the urine - Abdominal discomfort - Pain at the site of injection
Uncommon May affect up to 1 in 100 people	- Allergic reactions such as oedema of the face, urticaria - Feeling flushed - abdominal pain - Feeling numb - feeling dizzy - headache - tingling - venous clot
Rare May effect up to 1 in 1000 people	- lowering of blood pressure - cardiac arrest - chest pain - breathing difficulties - severe allergic reaction
Very Rare May affect up to 1 in 10000 people	- fatal anaphylactic reaction - myocardial infarction - collapse of cardiovascular system - convulsion - laryngeal oedema - pulmonary oedema - angina pectoris

Discussion

During the extrapolation of the data, we used the RGB scale. It defines a color space in terms of three components: Red, which ranges from 0-255; Green, which ranges from 0-255; and Blue, which ranges from 0-255. Combining red, green, and blue light is the standard method of producing color images on screen, such as TVs, computer monitors and smartphone screens.

The RGB color model is an additive one. In other words, Red, Green and Blue values (known as the three primary colors) are combined to reproduce other colors. When 100% of each color is mixed together, it creates white light. When 0% of each color is combined, no lights is generated, creating black.

The number of color supported by RGB depends on how many possible values can be used for red, green and blue. This is known as “color depth” and is measured in bits. The most common color depth is 24-bit color, also known as “true color”. It supports eight bits for each of the three colors, or 24 bits total. This provides 2^8 or 256 possible values for red, green and blue.

When displaying a color image on a screen, each pixel has a specific RGB value. In a 24-bit color, this value is between 0 and 255, where 0 is no color and 255 is full saturation.

We defined 2 main areas: the fluorescent and non-fluorescent. The sample for the fluorescent area is the dura mater. It is known that it has no BBB so it is always fluorescent. The sample of the control area

is the healthy parenchyma. Sometimes it may have a yellowish color due to the yellow microscope filter.

The maximum fluorescent value is found in the dura with a RGB mean value of 188; 241; 23.

The fluorescent tissue ranges from 255,255,250 as a maximum value to 0,68,3 in the minimum value.

In the control area we founded as maximum value 255, 158, 255 and minimum value 13,4,0; but we must consider that the visualization of the color is the three-channel combination.

At the margins of the tumor, we found a slowly decrease of the fluorescence until we have reached the final surgical cavity, after surgical removal of the lesion. In this area the mean values for the 3 channels are 129,149,47. In this area we must consider a residual fluorescence owing to the uncoagulated vessels and the manipulation of the tissue (Fig.12).

Fig. 12 Surgical cavity with a residual of fluorescein uptake by the tissue due to uncoagulated vessels.

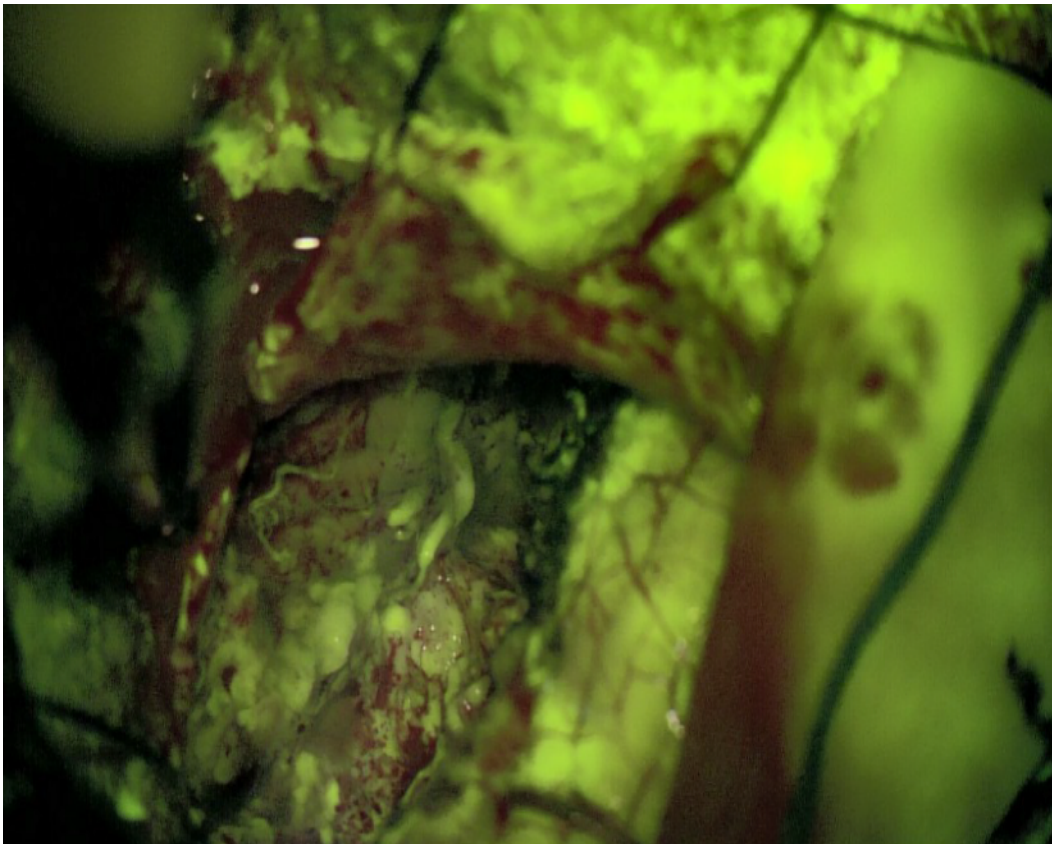

The main difference between the 2 surgical techniques is that the blue channel value is higher with the lighted Spetzler Suction Tube.

The surgical removal of the lesion is performed following the green tissue. Particular interest is given to the final stage, in order to evaluate tumor margins and “hidden corners” of surgical cavity (Fig. 13-14-15). In this stage we can find the Spetzler suction tube easier to use because with this device we can bring the light coaxial to the

surgical cavity improving better visualization of the residual tumor tissue.

Fig. 13 Surgical cavity

A. under white light the surgical cavity seems clean from pathological tissue.

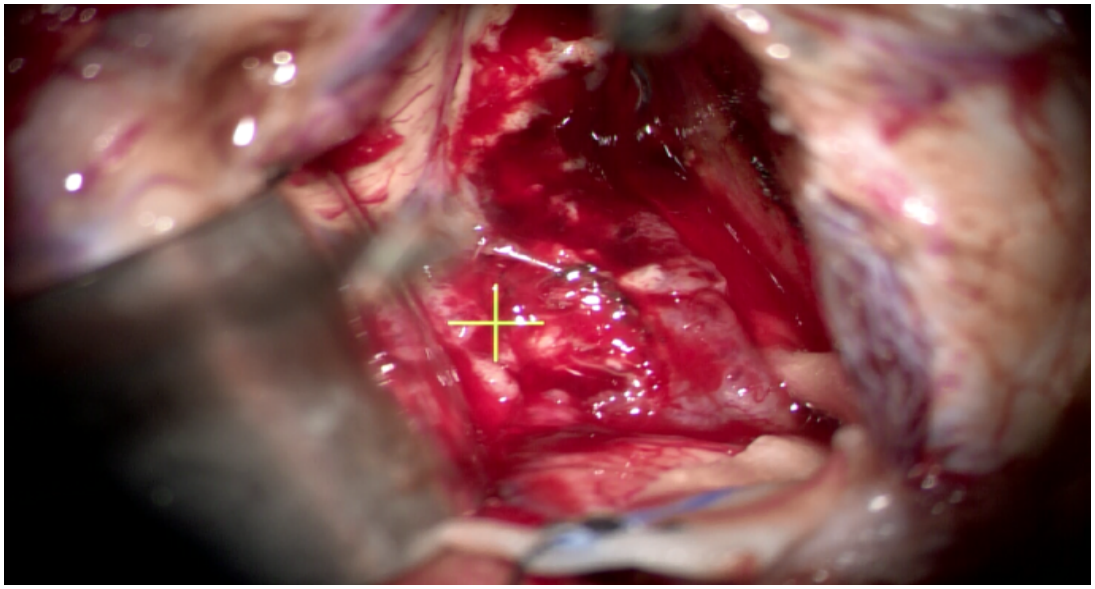

B. Under yellow light the remnant of the lesion is clear.

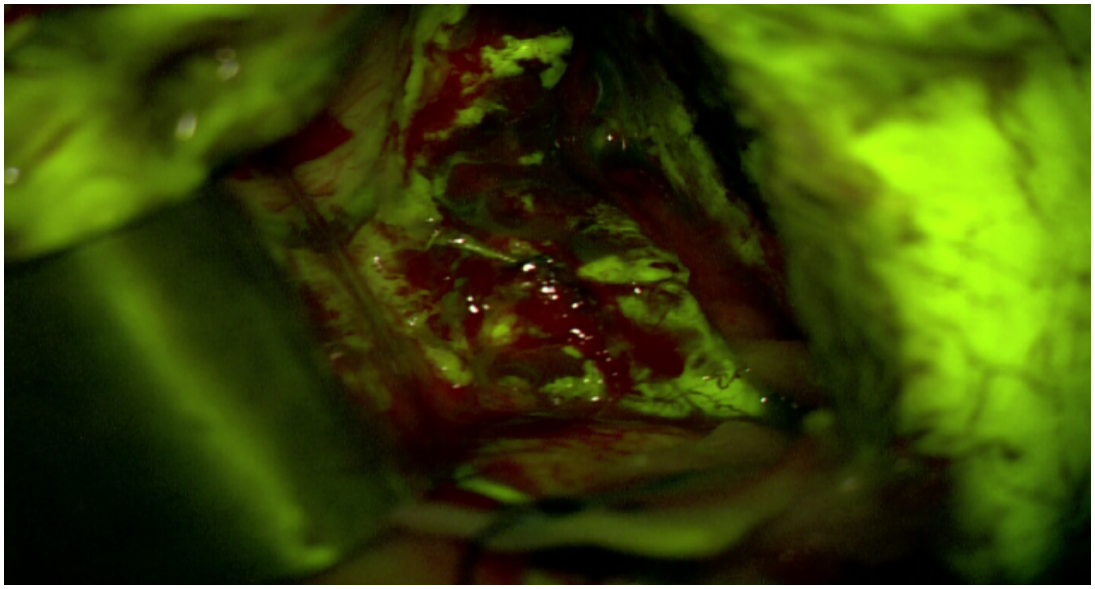

Fig. 14 Surgical cavity under white light in A, during hemostasis. In B, after hemostasis control of the surgical cavity with residual fluorescence due to a lesion remnant.

A. White light

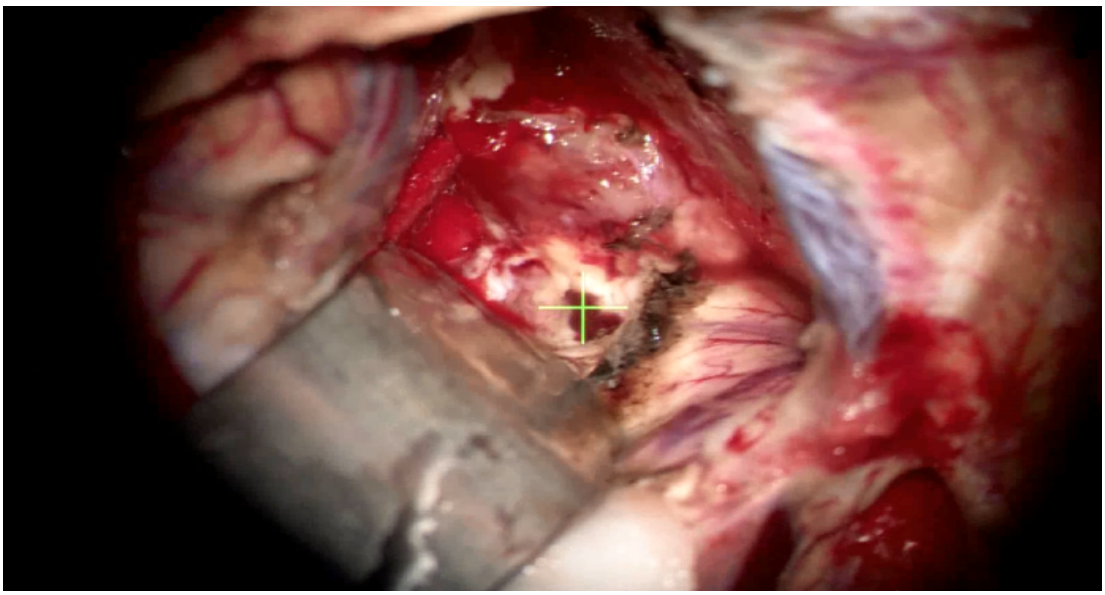

B. Yellow light with 560 filter.

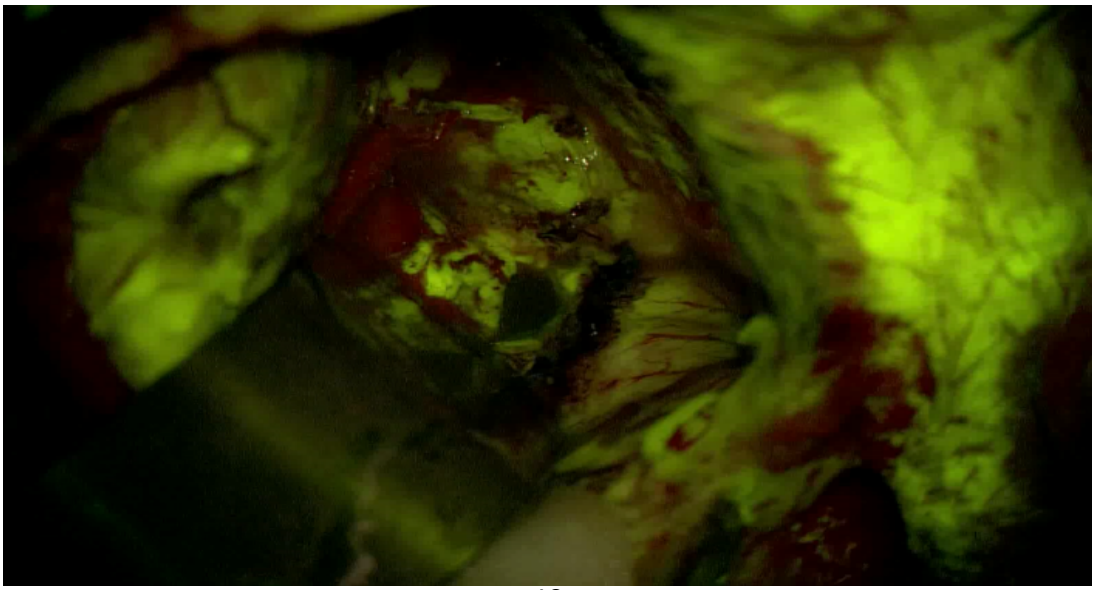

Fig. 15 Surgical cavity, “hidden corner”.

A. Under white light

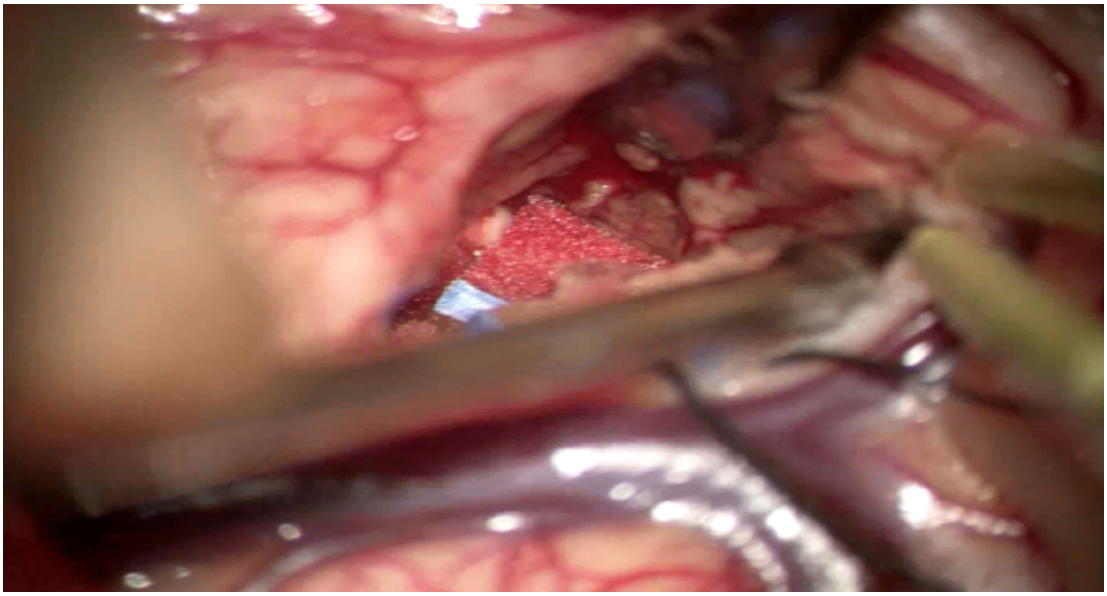

B. With yellow 560 filter residual fluorescent tissue is easier to find

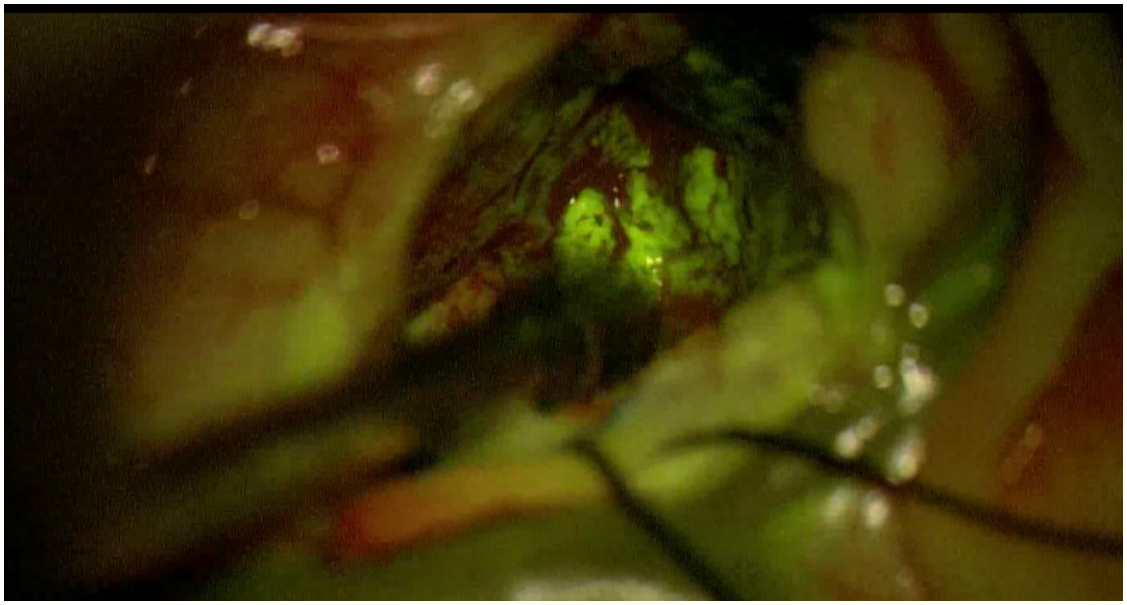

Following completion of resection, no further significant fluorescence is noted (Fig.16).

Fig.16 Surgical cavity at the end of surgery.

A. under white light at the final stage after hemostasis

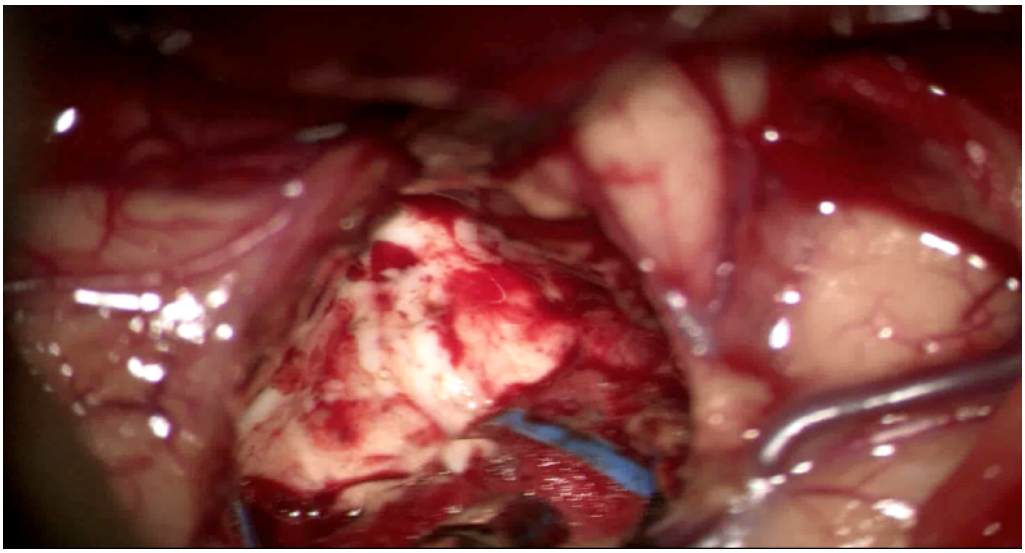

B. Under yellow 560 light no residual fluorescent staining.

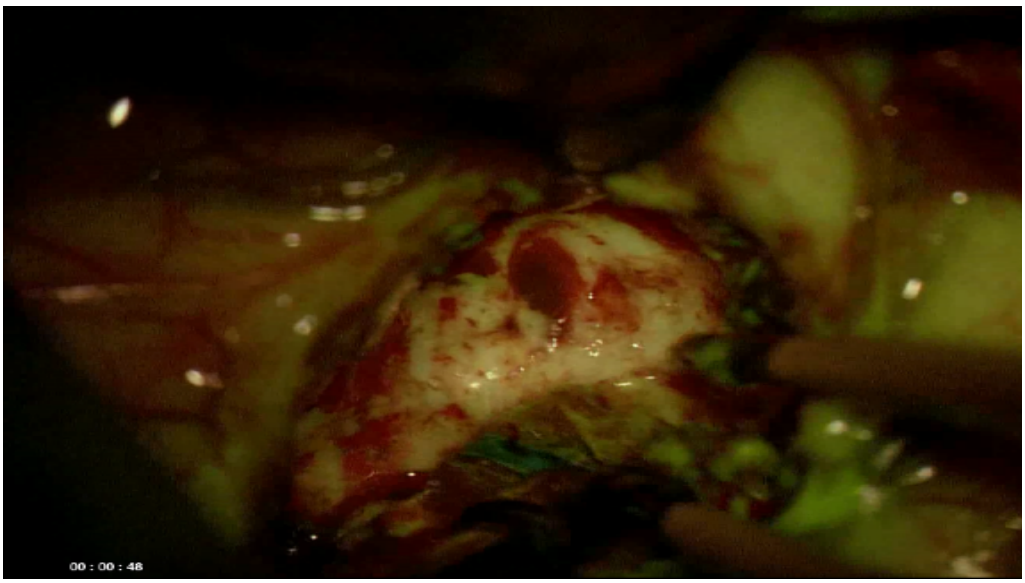

Sometimes a small amount of staining around cortical edges was related to breakdown of BBB due to bipolar coagulation (Fig. 17).

Fig. 17 In this figure at the final stage there is fluorescent uptake in cortical edges due to tissue manipulation

A. Under yellow light

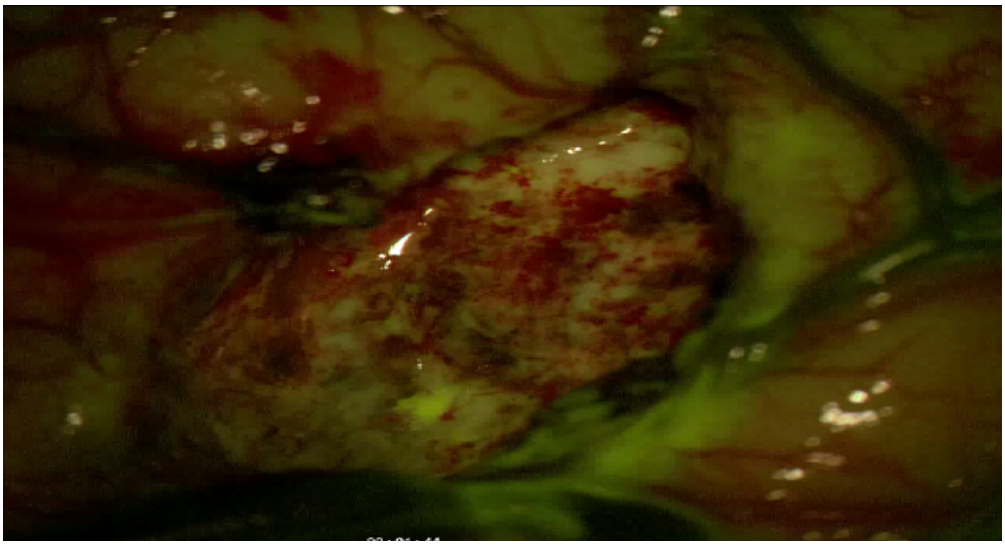

B. Under White light

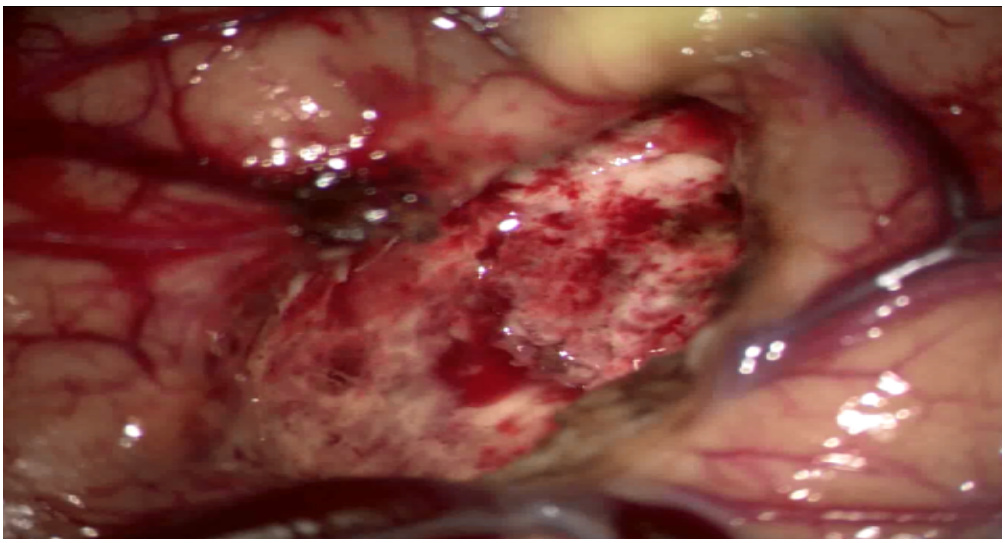

During and after surgery patients are closely followed-up for possible side effects related to the use of Fluorescein with clinical and biochemical parameters, including evaluation of arterial blood pressure, heart rate, O2 saturation, temperature, skin color and blood creatinine, as indicated by AIFA. The Fluorescein was well tolerated. Only 2 patients had an increased arterial blood pressure about 2 minutes from the intravenous injection.

Our results, about the use of fluorescein, considering the technique and the tumoral resection, are aligned with the literature. The surgeon classification of intraoperative fluorescence visualization between different lesion in our experience is similar to other works[34,35,36].

I In the work of Falco et alt. about the application of Fluorescein in Cranial and Spinal Tumors, the intensity of fluorescein was graded by the surgeon, considering the brightness and homogeneity. They found differences between different Histologies . Metastases, oligodendrogliomas and astrocytomas showed a heterogeneous intensity of fluorescence. Ependymomas, meningiomas, lymphomas sellar tumors and tumors of cranial and spinal nerves showed homogeneous and high intensity fluorescence. In their work they found that fluorescein is a good adjunct in every CSN tumor with BBB disruption proved by Gadolinium uptake[34].

In a similar fashion Acerbi et alt. classified the intensity of fluorescence in intramedullary tumors[35] and Vetrano et alt. classified peripheral nerve lesions[36]. As in their work we found bright and homogeneous fluorescence in ependymomas. The fluorescence was

absent in grade II astrocytomas and benign glioneuronal tumors. All these findings corresponding to the enhancement in MRI.

At the moment there are few works about objective fluorescein intensity and histological pattern of lesion[23,37].

In 2017 Neira at al correlated intraoperative fluorescein staining with histopathological alteration in contrast enhancing and non-contrast enhancing intracranial Glioblastoma. They found high intensity fluorescence in contrast enhancing tissue containing frank tumor cells. Notably, fluorescence was also found in non-contrast enhancing regions in many tumors which may be due to different vascularization or inflammation and have been considered tumor positive and targeted for resection when safe and possible. Necrotic regions exhibited variable levels of fluorescence, from bright to none[23].

In their work Kuroiwa et al histologically examined GBM specimens collected at autopsy or during surgery. They found a gradual increase in the number of tumor cells from the normal brain tissue around the tumor toward the main portion of the tumor. Cellular density in the periphery was low, with a few tumor cells scattered among normal cells. Walls of blood vessels in this region were conspicuous due to reactive astrocytes, but no histological changes were found in the vascular wall itself. In the tissue with high tumor cell density, which appeared to be the main portion of the tumor, the so-called endothelial proliferation was noted. The density of blood vessels decreased toward the tumor center, and blood vessels with a thick wall and a small caliber and thin wall with large caliber were present. In the central necrotic tissue, necrosis of both tumor cells and vascular cells

occurred. In the histological examination, the regions showing intense fluorescence were rich in tumor cells and showed a strong vascular reaction, whereas the regions of necrosis or with less tumor cells and without vascular reaction around the tumor showed no fluorescence. In the regions where tumor cells were dense, and could have been the main portion of the tumor, the vascular reaction was strong and the fluorescent dye have leaked out. In the region around that, a low tumor cell density and little or no vascular reaction were found, and no leak of fluorescent dye would have been expected[37].

As previously postulated, Na-Fl uptake in the extracellular space is the result of disruption of BBB[15]. This means that Na-Fl accumulates in the same areas of gadolinium enhancement on MRI. However, in 2018, Schebesch et al showed that non-gadolinium enhancing gliomas revealed an intraoperative yellowish stain during resection. So intraoperative detection and border zone identification of the gliomas was possible. These lesions had strong metabolic activity at FET-PET study [38].

The utility of Na-Fl in neurosurgery is well known. The first use was in high-grade gliomas and glioblastoma to optimize the extent of resection. Shinoda et al presented a series of 32 patients with glioblastoma for whom resection was guided by high-dose Na-Fl (20 mg/kg)[39]. With the advent of specific microscope filters to optimize visualization, low doses of Na-Fl was utilized[3,4,37,40,41,42]. The usefulness of Na-Fl is well established even in recurrent glioblastoma in literature such as in our experience. Hoehne et al found a good intraoperative fluorescence in 106 recurrent GBM, and this

fluorescence had no difference between primary GBM and recurrent one. In addition they have not found Na-Fl uptake in scar tissue[43]. The fluorescein uptake was variable in our experience such as the experience of Schebesch et al the fluorescent effect was pronounced in vital tumor margins and was absent in the necrotic part; although the fluorescent was heterogeneous in many cases, it still allow a clear delineation of tumor margins[42]. Our findings on G values in WHO grade IV lesions was from 197 and 230.

We used this technique for metastases removal as confirmed by previous study. The complete resection of metastases has been shown to benefit patients and to be crucial for quality of life and the efficacy of subsequent treatments. In these works Na-Fl makes the surgery easier, identifying the target area, resulting in a higher resection rate [22,34,44,45,45,47,48].

The value of Fluorescein is similar to the high-grade glioma with a maximum value of G 250, and a minimum value of G150. The uptake was inhomogeneous and the intensity was from moderate to intense as described in other works [45]. We can postulate that the high intensity was related to high cellularity and the lower intensity was related to cellular necrosis.

The importance in the treatment of metastases is that the follow-up is different.

In their work Okuda et al Fluorescence-guided surgery with gross total resection in cerebral metastases, achieved successful local control in 80% of patients with no Whole Brain RadioTherapy (WBRT). Statistical analysis revealed that additional WBRT tended to improve the local recurrence rate, but not significantly. In their study FGS

postpones the subsequent WBRT but also keeps WBRT as a therapeutic option for subsequent cerebral metastases. This prolongs survival and decrease the rate of central nervous system death. In their study they found no difference in staining intensity among the metastases of different types of primary Cancer[44].

To our knowledge, De Silva et al first published their surgical results of Na-Fl guided resection of extra axial tumors (1 craniopharyngioma, 1 vestibular schwannoma, 1 pituitary adenoma, 3 meningiomas) after injection of high dose of Na-Fl under white light illumination[49,50]. The same group provided a report on 5 frontal convexity meningiomas resected after injection of high NA-Fl doses (1000 mg of 20%)[51]. Akcakaya et al performed meningioma surgery in 30 patients with NA-Fl. They have found that this dye was useful in demonstrating the cleavage between brain tissue and the tumor, but also, according to vascular protocol of Na-Fl, to evaluate Na-Fl stained vessels for patency and to understand the relationship with the tumor(feeder/en passage vessel, perforating vessels, drainage veins). This approach helps to avoid vascular injury during surgery that is associated with postoperative morbidity. In addition, they have found Na-Fl particularly helpful to follow meningioma tissue within hyperostotic bones at the skull base and calvarium[52]. Fluorescent staining in our study is bright and homogeneous. G values ranged between 182 and 215.

In our research, we performed peripheral nerve surgery with this technique. We removed 2 vestibular schwannomas, 4 peripheral nerve schwannomas and 2 spinal schwannomas, with a high intensity

of fluorescence, G from 131 to 255. The use of fluorescein during schwannomas surgery was described in other works [36,53,54].

The utility of Na-Fl in vestibular schwannomas was showed in the work of Perez in 2018 demonstrating that merlin-deficient Schwann cells and vestibular schwannoma cells had higher uptake of Na-Fl than normal primary Schwann cells[31].

Pedro et al. described fluorescein use during resection of benign peripheral nerve sheath tumors[55]. Other use in peripheral nerve surgery was described by Stone et al. during surgery for peroneal intraneural ganglion cysts. They chose Fluorescein as the fluorophore for their case because of its propensity to highlight abnormal structures within the nervous system. In fact the nerve injury caused by pressure from the dissecting cyst likely leads to increased endoneurial vessel permeability and therefore enhanced appearance during visualization with the yellow microscope filter[56]. Even though Falco in his work found no difference between the lesion and the nerve[34], in our research we found useful use of the fluorescein; with a good illumination of the surgical field, we can discriminate between the green-yellow appearance of the lesion and white-grey appearance of the nerve. In the work of Vetrano et alt. the surgeons needed to lower the Na-Fl dosage to 1 mg/kg to better discriminate the difference between nerve and lesion. With their technique they found useful use of fluorescein in schwannomas, neurofibromas because of their homogeneous and intense fluorescence. In mixoma and other malign lesion fluorescein was not useful to remove the lesion, in fact their intensity was slight and inhomogeneous[36].

As in other works the first look under yellow filter showed only a slightly higher fluorescence zone corresponding to the tumor; after tumor pseudocapsule opening the real difference between tumor and normal fibers was observed[36,53,54,57].

Little is known about how fluorescein accumulates in peripheral nervous tissue. Abram et al. used fluorescein as a hydrophilic marker to study how nerve injury affects dorsal root ganglia permeability. In this study they demonstrated that after 30 minutes fluorescein appeared in damaged peripheral nervous tissue following intravenous, intrathecal, epidural or epineural injection. With intravenous injection, the control animals exhibited high uptake in the dorsal root ganglion and low uptake into the sciatic nerve. After nerve injury, they found a dramatic increase in fluorescein uptake in the sciatic nerve and high fluorescein content surrounding individual fascicles. This increase in intraneural dye was attributed to an increased permeability of the peripheral nerves[58]. In a separate sciatic nerve injury model, an increase in permeability of endoneurial blood was detected, despite a preserved ultrastructural appearance. This was associated to a concomitant increase in number of mast cells, which may provide an explanation of the dye accumulation[59].

In their works Pedro et al described the utility of Na-Fl during peripheral nerve sheath tumor surgery, 10 cases of schwannomas[53]. In 2020 Pedro et al described the intraoperative use of Na-Fl for identification of the target fascicle for biopsy; in fact they found enhanced tissue differentiation between normal and pathological fascicles, leading to more limited and accurate biopsy[54].

Despite these previous works, Kalamarides et alt considered that Na-Fl added limited additional value in primary peripheral nerve schwannoma. They found it useful only in one case to discriminate the lesion from the normal nerve. Na-Fl did not help with the safe entry zone in the psuedocapsule incision. In addition during intraneural dissection the colorimetric variation between tumor and normal tissue induced by fluorescence did not outperform the natural contrast between the yellow true capsule and the gray-red layers of the pseudocapsule[57].

In our study, we have found that the fluorescence intensity is different for the different lesions and it's different during the same surgery. From our experience, we can also postulate that this intensity decreases as the distance from the light source and detector increases from the interrogated area. The collected light is dependent on numerous factors including the amount of excitation light, tissue optical properties, time from the administration of the dye, surgical manipulation of the tissue, necrosis area and perilesional edema[60].

Our results provide strong evidence that intraoperative Na-Fl is a safe and reliable indicator of pathological tissue in CNS and PNS. Fluorescein is useful for guiding safe and when possible, radical resection of the tumor. This might improve progression free survival and overall survival.

Our operative threshold curves determining the value of accuracy were found at 167G under which the probability of finding malignant cells is lower (Fig.11 B).

Conclusion

In this project we found an intrinsic threshold that has an influence on diagnostic accuracy. This could highlight all brain tissue to a certain extent, despite having higher concentration in tumor tissue and in the dura. This threshold will have to be clearly described. Increasing the threshold will lead to fewer false negatives and lowering the threshold will lead to more false positives. Thus, defining a threshold will directly affect diagnostic accuracy. Optimally, receiver operating curves should be employed to relate all thresholds to their respective diagnostic accuracy[61].

We must keep in mind that the intraoperative signal can change. During a neurosurgical procedure lasting several hours, the signal induced in tissue will change over time. While fluorescein has no specific affinity to tumor cells, concentrations are at first high in perfused tissue and are later extravasated in tumor matrix, leading to pseudoselectivity. However, there is some concern about unspecific propagation with edema[15,62].

The intensity of this value is important because there are no more malignant cells. The minimum intralesional value for G where we can find positive histology is 167. Below this value we can postulate there are no malignant cells, or no cell (necrotic area).

At this moment we found differences between different types of tissue in the green channel but no significant difference in the R and B channels. In fact there is a wide range of variability in this channels because of the presence of blood, microscope light and instrument

shadow on the parenchyma. We need more data to complete the research in the R and B channels.

Future work

Our data can be used in future research. The threshold found could be associated with the microscope yellow software to calculate the Fluorescein intensity during surgery to obtain a 360° use of Fluorescein. The surgeon can see on the microscope ocular the fluorescein intensity to continue removing lesion or stop it.

We found differences between different histological tissue about green intensity and characteristics but further work is necessary to perform a statistical analysis.

This work can also be a starting point to find correlation with intratumoral markers and intensity of fluorescein. As described before, the color is a combination of RGB values, so we can also compare the combination of the 3 elements together to have the complete color values in the pathological tissue.

References

1.Xia T, Li N, Fang X. Single molecule fluorescence imaging in living cells. Annu Rev Phys Chem 2013;64(1):459-480

2.ZhangD,Singhal S, Lee J. Optical Principles of Fluorescence guided brain tumor surgery: a practical primer for the Neurosurgeon. Neurosurg. 2019, 85:312-324

3.Acerbi, Broggi, Schebesch et al. Fuorescein guided surgery for resection of high-grade gliomas: a multicentric prospective phase II study (FLUOGLIO). Clin. Cancer Res, 2018; 24(1): 52-61

4.Schebesch KM, Brawanski A, Hohenberger C, Hohne J Fluorescein Sodium-Guided Surgery of Malignant Brain Tumors: History, Current Concepts, and Future Project Turk Neurosurg. 2016;26(2):185-94

5.Zhang RR, Schroeder AB, Grudzinsky JJ et al. Beyond the margins: realtime detection of cancer using targeted fluorophores. Nat Rev Clin Oncol. 2017; 14(6):347-364

6.Lavis LD, Rainers RT, Bright ideas for chemical biology. ACS Chem Biol. 2008;3:142-155

7.Chen RF, Knutson JR. Mechanism of fluorescence concentration quenching of carboxifluorescein in liposomes: energy transfer to non-fluorescent dimers. Anal Biochem. 1988;172:61-77

8. Lakowicz JR**,** Principles of fluorescence spettroscopy. 2006. doi 10.1007/978-0-387-46312-4.

9. Zhao T, Huang G, Li Y, et al. A transistor like pH nanoprobe fot tumor detection and image-guided surgery. Nat Biomed Eng 2016:6-14.

10.Savariar EN, Felsen CN, Nashi N, et al. Real time in Vivo molecular detection of primary tumors and metastases with ratiometric activatable cell-penetrating peptides. Cancer Res 2013:73:855-864

11.Zheng Q, Lavis LD, development of photostable florophores for molecular imaging. Curr OpinChem Biol 201739: 32-38

12.Richards-Kortum R, Sevick-Muraca E. Quantitative optical spectroscopy for tissue diagnosis. Ann Rev Phys Chem 1996;47:555-606

13.Martirosyan NL, Eschbacher JM, Kalani MYS, et al. Prospective evaluation of the utility of intraoperative confocal laser endomicroscopy in patients with brain neoplasms using fluorescein sodium: experience of 74 cases. Neurosurg Focus. 2016; 40: E11-1-E11-8.

14.Raza SM, Banu MA, Donaldson A, Patel KS, Anand VK, Schwarz TH.Sensitivity and specificity of intrathecal fluorescein and white light excitation for detecting intra-operative cerebrospinal fluid leak in endoscopic skull base surgery. J Nurosurg. 2015;122: 1360-1369

15.Diaz RJ, Dios RR, Hattab EM et al. Study of biodistribution of fluorescein in glioma-infiltrated mouse brain and histopathological correlation of intraoperative findings in high grade gliomas resected under fluorescein fluorescence guidance. J. Neurosurg 2015;122(6):1360-1369

16.Pogue BW, Gibbs-Strauss S, Valdes PA et al. Review of Neurosurgical fluorescence imaging methodologies. IEEE J Sel Top Quantum Electron 2010; 16: 493-505

17.Abbott NJ, Ronnback L, Hansson E: Astrocyte-endothelial interactions at the blood-brain barrier. Nature reviews. Neuroscience 7(1):41-53, 2006

18.Kozler P, Pokorny J. Physiol. Altered Blood-Brain Barrier Permeability and Its Effect onthe Distribution of Evans Blue and Sodium Fluorescein in theRat Brain Applied by Intracarotid Injection. Res. 52: 607-614, 2003

19.Abbot N,J, Patabendige AA, Dolman DE, Yusof SR, Begley DJ Structure and function of the blood-brain barrier. Neurobiol Dis 2010; 37:13-25

20.Mastorakos P, McGavern D. The anatomy and immunology of vasculature in the central nervous system. Sci Immunol. 2019 Jul 12;4(37):eaav0492

21. Hendricks BK, Cohen-Gadol AA, Miller JC Novel delivery methods bypassing the blood-brain barrier and blood tumor barriers. Neurosurg Focus. 2015 Mar;38(3):E10

22.Ulrich H. WEIDLE, JENS NIEWÖHNER and GEORG TIEFENTHALER The Blood–Brain Barrier Challenge for the Treatment of BrainCancer, Secondary Brain Metastases, and Neurological Diseases CANCER GENOMICS & PROTEOMICS 2015,12: 167-178

23 Neira JA, Ung TH, Sims JS, Malone HR, Chow DS, Samanamud JL, Zanazzi GJ, Guo X, Bowden SG, Zhao B, Sheth SA, McKhann GM 2nd, Sisti MB, Canoll P, D'Amico RS, Bruce JN. Aggressive resection at the infiltrative margins of glioblastoma facilitated by intraoperative fluorescein guidance.J Neurosurg. 2017 Jul;127(1):111-122.

24. Folaron M, Strawbridge R, Samkoe K.S, Filan C, Roberts DW, Davis SC. Elucidating the kinetics of sodium fluorescein for fluorescence guided surgery of glioma. J.Neurosurg 2018 Sept.131(3): 724-734

25. Ichioka T, Miyatake S, Asai N, Kajimoto Y, Nagakawa T, Hayashi H et al. Enhanced detection of malignant glioma xenograft by fluorescein-human serum albumine conjugate. J. Neurooncol 2004, 67:47-67

26. Sun H, Dennis R. Johnson, Rick A. Finch, Alan C. Sartorelli, Donald W. Miller, and William F. Elmquist Transport of Fluorescein in MDCKII-MRP1 Transfected Cells and mrp1-Knockout Mice1Haiying, Biochemical and Biophysical Research Communications 284, 863–869 (2001)

27.Olsson Y. Microenvironment of te peripheral nervous system under normal and pathological conditions. CRIT. Rev.Neurobiol 1990;5:265-311

28. Ouyang X, Dong C, Ubogu EE: in situ molecular characterization of endoneurial microvessels that form the blood-nerve-barrier in normal human adult peripheral nerves. J.PeripherNervSyst 2019;24:195-206

29. Richner M, Ferreira N, Dudele A, Jensen TS, Vaegter CB, Goncalves NP. Functional and structural changes of the blood-nerve-barrier in diabetic neurophaty. Front Neurosci 2019;12:1038

30. Malmgre LT, Olsson Y. Differences between the peripheral and the central nervous system inpermeability to sodium fluorescein. 1980; 191(1):103-107

31. Perez ER, Brachop O, Ein L, Szczupak M, Monje PV, Fernandez-Valle C, et alt Fluorescent detection of Merlin-deficient Schwann cells and primary human vestibular schwannoma cells using sodium fluorescein. Otol Neurotol 2018;39:1053-1059

32. Bolton SJ, Anthony DC, Perry VH. Loss of the thigh junctions proteins occludin and zonula occludens-1 from cerebrovascular endothelium during neutrophil-induced blood-brain-barrier breakdown in vivo. Neuroscience 1998; 86:1245-1257

33. Acerbi F, Broggi M, Broggi G, Ferroli P. What is the best timing for fluorescein injection during surgical removal of high-grade gliomas? Acta Neurochir 2015,157:1377-1378.

34. Falco J. Cavallo C, Vetrano IG, De Laurentis C, Siozos L, Schiariti M, Broggi M, Ferroli P, Acerbi F. Fluorescein application in cranial and spinal tumors enhancing at preoperative MRI and operated with a dedicated filter on the surgical microscope: preliminary results in 279 patients enrolled in the FLUOCERTUM prospective study. Frontiers in Surg. 2019; 6:1-13

35. Acerbi F, Cavallo C, Schebesch KM, Akçakaya MO, de Laurentis C, Hamamcioglu MK, Broggi M, Brawanski A, Falco J, Cordella R, Ferroli P, Kiris T, Höhne J Fluorescein-Guided Resection of Intramedullary Spinal Cord Tumors: Results from a Preliminary, Multicentric, Retrospective Study.World Neurosurg. 2017 Dec;108:603-609

36. Vetrano IG, Acerbi F, Falco J, Devigili G, Rinaldo S, Messina G, Prada F, D'Ammando A, Nazzi V. Fluorescein-guided removal of peripheral nerve sheath tumors: a preliminary analysis of 20 cases.J Neurosurg. 2019 Dec 6:1-10.

37. Kuroiwa T, Kajimoto Y, Ohta T. Comparison between operative findings on malignant glioma by a fluorescein surgical microscopy and histological findings. Neurol Research 1999;21:130-134.

38. Schebesch KM, Brawanski A, Doenitz C, Rosengarth K, Proescholdt M, Riemenschneider MJ, Grosse J, Hellwig D, Höhne J.Fluorescence-guidance in non-Gadolinium enhancing, but FET-PET positive gliomas Clin Neurol Neurosurg2018 Sep;172:177-182

39. Shinoda J, Yano H, Yoshimura S, Okumura A, Kaku Y, Iwama T, Sakai N. Fluorescence-guided resection of glioblastoma multiforme by using high-dose fluorescein sodium. Technical note. J Neurosurg. 2003 Sep;99(3):597-603

40. Acerbi F, Broggi M, Eoli M, Anghileri E, Cavallo C, Boffano C, Cordella R, Cuppini L, Pollo B, Schiariti M, Visintini S, Orsi C, La Corte E, Broggi G, Ferroli P. Is fluorescein-guided technique able to help in resection of high-grade gliomas? Neurosurg Focus. 2014 Feb;36(2):E5.

41. Acerbi F, Broggi M, Eoli M, Anghileri E, Cuppini L, Pollo B, Schiariti M, Visintini S, Orsi C, Franzini A, Broggi G, Ferroli P.Fluorescein-guided surgery for grade IV gliomas with a dedicated filter on the surgical microscope: preliminary results in 12 cases. Acta Neurochir (Wien). 2013 Jul;155(7):1277-1286

42. Schebesch KM, Proescholdt M, Höhne J, Hohenberger C, Hansen E, Riemenschneider MJ, Ullrich W, Doenitz C, Schlaier J, Lange M, Brawanski A Sodium fluorescein-guided resection under the YELLOW 560 nm surgical microscope filter in malignant brain tumor surgery--a feasibility study. Acta Neurochir (Wien). 2013 Apr;155(4):693-699

43. Höhne J, Schebesch KM, de Laurentis C, Akçakaya MO, Pedersen CB, Brawanski A, Poulsen FR, Kiris T, Cavallo C, Broggi M, Ferroli P, Acerbi F.Fluorescein Sodium in the Surgical Treatment of Recurrent Glioblastoma Multiforme. World Neurosurg. 2019 May;125:e158-e164

44. T.Okuda, K.Kataoka, T.Yabuuchi, H.Yugami, A.Kato Fluorescece-giuded surgery of metastatic brain tumor using fluorescein sodium J. of Clinical Neurosc. 17(2010):118-121

45. Schebesch KM, Hoehne J, Hohenberger C, Proescholdt M, Riemenschneider MJ, Wendl C, Brawanski A. Fluorescein sodium-guided resection of cerebral metastases-experience with the first 30 patients. Acta Neurochir (Wien). 2015 Jun;157(6):899-90

46. Rey-Dios R, Cohen-Gadol AA. Technical principles and neurosurgical applications of fluorescein fluorescence using a microscope-integrated fluorescence module Acta Neurochir (Wien) 2013 Apr;155(4):701-6

47. Xiao S, Zhang J, Zhu Z, Li Y, Zhong W, Chen J, Pan Z, Xia H. Application of fluorescein sodium in breast cancer brain metastasis surgery. Cancer Manag Res. 2018 Oct 12;10:4325-4331

48. Höhne J, Hohenberger C, Proescholdt M, Riemenschneider MJ, Wendl C, Brawanski A, Schebesch KM. Fluorescein sodium-guided resection of cerebral metastases-an update. Acta Neurochir (Wien). 2017 Feb;159(2):363-367

49. Da Silva CE, da Silva JL, da Silva VD. Use of sodium fluoresceinin skull base tuors. Surg Neurol Int. 2010; 1:70

50. Da Silva CE, da Silva, da Silva JL. Sodium Fluorescein in skull base meningiomas: a technical note. Clin Neurol Neurosurg. 2014; 120:32-35

51. Da Silva CE, da Silva, da Silva JL. Convexity meningiomas enhanced by sodium fluorescein. Surg Neurol Int 2014, 5:3

52. Akçakaya MO, Göker B, Kasımcan MÖ, Hamamcıoğlu MK, Kırış T. Use of Sodium Fluorescein in Meningioma Surgery Performed Under the YELLOW-560 nm Surgical Microscope Filter: Feasibility and Preliminary Results.World Neurosurg. 2017 Nov;107:966-973

53. Pedro MT, Eissler A, Schmidberger J, Kratzer W, Wirtz CR, Antoniadis G, Koenig RW Sodium Fluorescein-Guided Surgery in Peripheral Nerve Sheath Tumors: First Experience in 10 Cases of Schwannoma. World Neurosurg. 2019 Jan 17:S1878-8750(19)30079-8. doi: 10.1016/j.wneu.2019.01.010. Online ahead of print

54. Pedro MT, Eissler A, Scheuerle A, Schmidberger J, Kratzer W, Wirtz CR, Antoniadis G, Koenig RW. Sodium Fluorescein as Intraoperative Visualization Tool During Peripheral Nerve Biopsies. World Neurosurg. 2020 Jan;133:e513-e521. doi: 10.1016/j.wneu.2019.09.081. Epub 2019 Sep 21

55. Pedro M, Konig R, Antoniadis G. Fluorescein-guided surgery in peripheral benign nerve tumors (schwannomas). 2017. 6th Vienna Symp. Surg. Peripher. Nerves present state Peripher. Nerves surg. New Ideas to Improv.Results. Vienna p29

56. Stone JJ, Graffeo CS, de Ruiter GCW, Rock MG, Spinner RJ Intraoperative intravenous fluorescein as an adjunct during surgery for peroneal intraneural ganglion cysts. Acta Neurochir (Wien). 2018 Mar;160(3):651-654

57. Kalamarides M, Bernat I, Peyre M. Extracapsular dissection in peripheral nerve schwannoma surgery using bright light and fluorescein sodium visualization: case series. Acta Neurochir (Wien). 2019 Dec;161(12):2447-2452. Epub 2019 Nov 2.

58. Abram SE, Yi J, Fuchs, Hogan QH Permeability of injured and intact peripheral nerves and dorsal root ganglia. Anhestesiology 2006;105:146-153

59. Latker CH, Wadhwani KC, Balbo A, Rapaport SI. Blood nerve barrier in frog during wallerina degeneration: are axons necessary for maintenance of barrier function? J Comp Neurol 1991; 308: 650-664

60. Walter Stummer. Factors confounding fluorescein-guided malignant gliomare sections: edema bulk flow, dose, timing, and now: imaging hardware? Acta Neurochir (2016) 158:327–328

61. Florkowsky CM. Sensitivity, receiver-operating characteristic (ROC) curves and likelihood ratios: communicating the performance of diagnostic tests. Clin. Bioche. Rev 2008; 29(suppl1)S83-S87

62. Stummer W, Gotz C, Hassan A, Kempski O. Kinetics of photofrin II in perifoal brain edema. Neurosurgery 1993; 33(6): 1075-1081

Abbreviations

BBB Blood Brain Barrier

BNB Blood Nerve Barrier

CNS Central Nervous System

FGS Fluorescein Guided Surgery

GBM Glioblastoma Multiforme

HGG High Grade Glioma

HIF Hypoxia inducible factor

MRI Magnetic Resonance Imaging

Na-Fl Sodium Fluorescein

TJ tight junction

VEGF Vascular Endothelial Growth Factor

WBRT Whole Brain RadioTherapy